Design, synthesis, and biological characterization of proteolysis targeting chimera (PROTACs) for the Ataxia telangiectasia and RAD3-related (ATR) kinase

Abdallah M. Alfayomy[1,2,*], Ramy Ashry[3,4,*], Anita Kansy[3], Frank Erdmann[1], Matthias Schmidt[1], Oliver H. Krämer[3,¶], Wolfgang Sippl[1,¶]

1 Department of Medicinal Chemistry, Institute of Pharmacy, Martin-Luther-University of Halle-Wittenberg, 06120 Halle (Saale), Germany

2 Department of Pharmaceutical Chemistry, Faculty of Pharmacy, Al-Azhar University, Assiut, 71524, Egypt

3 Department of Toxicology, University Medical Center, Johannes Gutenberg-University Mainz, 55131, Mainz, Germany

4 Department of Oral Pathology, Faculty of Dentistry, Mansoura University, Mansoura 35516, Egypt.

* equal first author contribution

¶ equal last author contribution; correspondence to okraemer@uni-mainz.de or wolfgang.sippl@pharmazie.uni-halle.de

---

Abstract

The Ataxia telangiectasia and RAD3-related (ATR) kinase is a key regulator of the DNA replication stress responses and DNA-damage activated checkpoints. Several potent and selective ATR inhibitors are reported and four of them are currently in clinical trials in combination with radio- or chemotherapy. Based on the idea of degrading target proteins rather than inhibiting them, we designed, synthesized and biologically characterized a library of ATR-targeted proteolysis targeting chimera (PROTACs). Among the synthesized compounds, the lenalidomide-based PROTAC **42i** (Abd110) was the most promising when tested in pancreatic cancer cells (MIA PaCa-2). It reduced ATR to 40 % of the levels in untreated cells. **42i** (Abd110) selectively degraded ATR through the proteasome without affecting the associated kinases ATM and DNA-PKcs. **42i** (Abd110) may be a promising candidate for further optimization and biological characterization in various cancer cells.

Key words: Ataxia telangiectasia and RAD3-related (ATR) kinase, proteolysis targeting chimera (PROTAC), protein degradation, synthesis, MIA PaCa-2

1. Introduction

Chemotherapeutics induce DNA replication stress and DNA damage. If such lesions are not repaired, they cause cell death. Exogenously induced and endogenous DNA replication problems and DNA lesions activate checkpoint kinases, which slow down the cell cycle and initiate DNA repair [1-3]. The checkpoint kinases ataxia telangiectasia-mutated (ATM) and checkpoint kinase-2 (CHK2) are mainly activated in cells with double-strand DNA breaks. DNA replication stress, due to slow or blocked DNA replication forks and single-strand DNA breaks, activates Ataxia telangiectasia and RAD3-related (ATR) and checkpoint kinase-1 (CHK1). DNA-dependent protein kinase catalytic subunit (DNA-PKcs) is, like ATM and ATR, an apical checkpoint kinase immediately sensing DNA stress [2, 3].

The coordination of cellular responses to DNA replication stress and endangered DNA integrity by checkpoint kinase has propelled an intense search for pharmacological inhibitors of such enzymes [4, 5]. In particular, ATR kinase has attracted interest, as cancer cells are heavily rely on ATR to cope with the increased amount of replication stress, and also mutations in ATR are less common [3, 6, 7]. A first potent and selective inhibitor for ATR, **I** (VE-821), was reported by Vertex Pharmaceuticals [8]. The inhibitor is highly selective for ATR compared to its homologous kinases ATM and DNA-PK. Preclinical studies have shown that **I** (VE-821) is able to sensitize multiple tumor cell lines to various treatments, including cisplatin, ionizing radiation, gemcitabine, topoisomerase I poisons, etoposide, and oxaliplatin [9-11]. Although it was effective at inhibiting ATR, it lacked pharmacokinetic properties needed to advance into clinical trials [8, 12]. Several optimizations have been made on this scaffold to increase the potency and cellular activity against ATR and to improve its physicochemical properties. For instance, the isosteric replacement of the amide with a 1,3,4-oxadiazole moiety as in compound **II** increased the cellular activity against ATR [12]. Further modifications led to the discovery of another candidate **III (**VX-970, also known as VE-822**)** with improved potency, selectivity, and water solubility, which is currently in phase II clinical trials [12-14]. (Figure 1)

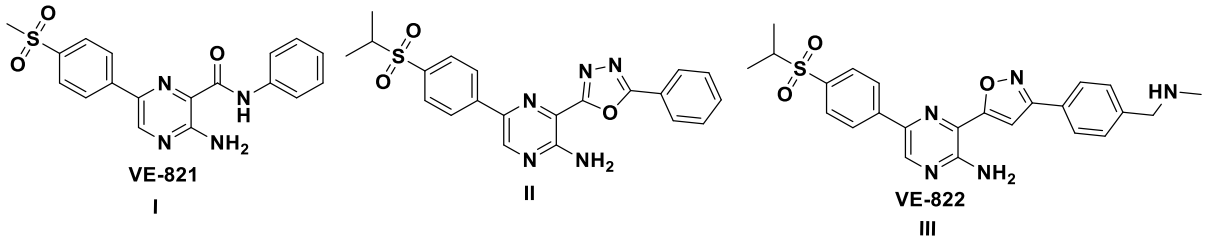

Figure 1: Examples of reported ATR inhibitors that were used in this work for the development of PROTACs.

Proteolysis targeting chimeras (PROTACs) have emerged as a highly promising new strategy for the development of future drugs [15-17]. These heterobifunctional molecules consist of a ligand which binds to the target protein of interest, a ligand binding to an E3 ubiquitin ligase (such as cereblon, CRBN, or von Hippel–Lindau tumor suppressor, VHL), and a linker connecting both ligands. PROTACs initiate the degradation of their targets by inducing the formation of a ternary complex with an E3 ligase. This directs the ubiquitination machinery close to the protein. The polyubiquitinated protein is consequently recognized and degraded by the 26S proteasome. Studies have shown several advantages of PROTACs over the corresponding small molecule inhibitors, including increased potency, rapid and sustained depletion of the targeted proteins, and enhanced selectivity in cells [18, 19]. Eighteen protein degraders are currently in phase I to III clinical trials for the treatment of tumor patients [20, 21]. So far, targeted protein degraders (TPDs) have not been reported for the checkpoint kinases ATR, ATM, DNA-PKcs, CHK1, and CHK2. Such compounds would represent an innovative pharmacology to dissect and therapeutically assess the catalytic and non-catalytic functions of these key molecular regulators [22]. Herein, we report the chemical synthesis and biological characterization of the first-in-class degraders for ATR kinase through the application of the PROTAC concept.

We started the design of ATR PROTACs based upon the ATR inhibitors **I,** its analog **II,** and **III.** The interaction between the three ATR inhibitors and a rationally designed PI3K-alpha mutant that mimics ATR (for which a crystal structure has been reported, PDB ID 5UL1) [23] (Figure 2) was analyzed. In the crystal structure **I** occupies the ATP binding site and forms two hydrogen bonds between the 2-aminopyrazine moiety and the hinge region while the alkyl sulphone group is located in the solvent-exposed region of the protein. Docking of **II** and the VE-822 analog **IV** gave a similar orientation of the 2-aminopyrazine

and sulphone groups. Based on the structural information the sulphone group is proposed as feasible tethering site for connecting a linker group. Additionally, different E3 ligase ligands such as several cereblon ligands (thalidomide, lenalidomide, and other glutarimides) and VHL-ligand were considered for the PROTAC development using different alkyl and PEG linkers with variant linker lengths (Figure 3).

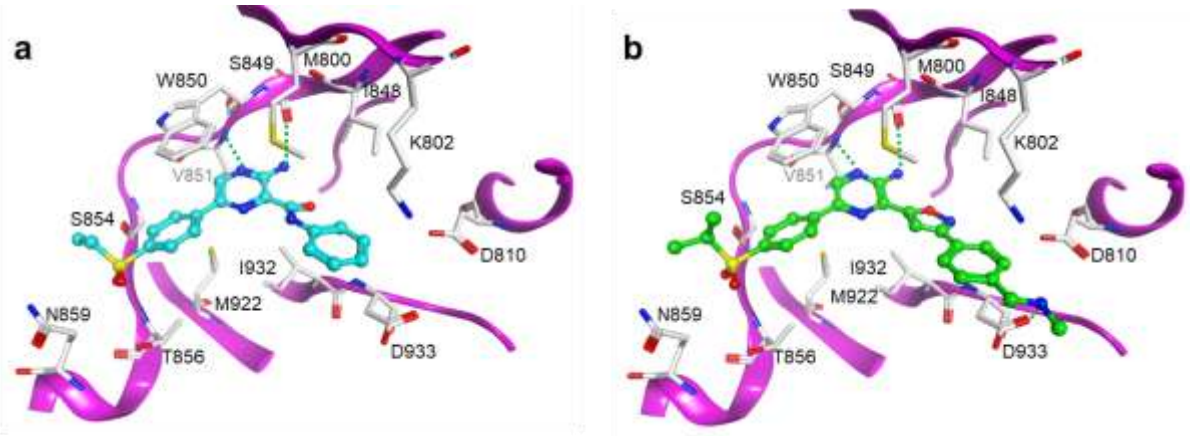

Figure 2: (A) Interaction of **I** (VE-821) and the ATR binding (rationally designed PI3K-alpha mutant that mimics ATR (PDB ID 5UL1) and obtained docking solution of **III** (VE-822)**.**

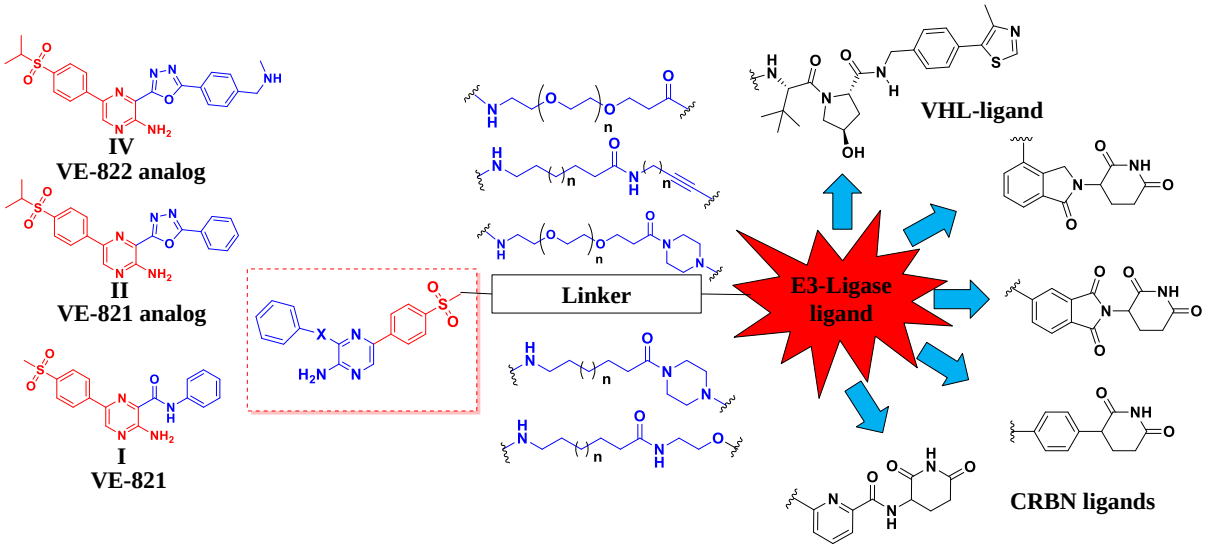

Figure 3: Strategy for Design of ATR PROTACs.

2. Results and discussion

2.1. Chemistry

The designed PROTACs were prepared via a convergent synthesis, including condensation between linker-connected ATR inhibitors (**12a-e** and **13a-f)** and different E3 ligase ligands (**20a-c, 25, 31, 35** and **41**), as outlined in Schemes 2-5. Also, the synthetic routes for the linker-connected ATR inhibitors were illustrated in Scheme 1. Firstly, the 4-bromobenzene sulfonyl chloride **2** reacted with different alkyl and PEG linkers **1a-f** to form the corresponding 4-bromobenzene sulfonamide derivatives **3a-f**. Secondly, 4-bromobenzene sulfonamides with alkyl linkers **3a-d** were converted to the corresponding boronates **4a-d** through the Miyaura borylation reaction by cross-coupling with bis(pinacolato)diboron [24]. Concurrently, ester hydrolysis of methyl 3-amino-6-bromopyrazine-2-carboxylate **8** with lithium hydroxide gives the corresponding acid **9** [8]. Then, the carboxylic acid group of the produced pyrazine carboxylic acid **9** either reacted with different benzohydrazides in the presence of triphenylphosphine and carbon tetrabromide to afford the 2-phenyl-1,3,4-oxadiazole derivative **10a, b** or was coupled with aniline through a HATU-mediated coupling reaction to form the corresponding carboxamide derivative **11a** [12, 25]. The benzohydrazide derivative **7,** which was required for the synthesis of the oxadiazole derivative **10b,** was synthesized starting from the corresponding substituted methyl benzoate **5** by *N*-methylation with methyl iodide in the presence of sodium hydride, followed by reaction with hydrazine hydrate in methanol, affording the corresponding benzohydrazide derivative **7**. Furthermore, the pyrazine carboxamide **11a** was converted to the corresponding pinacol boronic ester **11b** through the Miyaura borylation reaction [24, 26]. Finally, cross-coupling of bromoaryl intermediates **3e, 3f, 10a, b** and **11a** with the appropriate pinacolate boronic ester derivatives **4a-d** and **11b** using the Suzuki cross-coupling reaction followed by ester hydrolysis either by trifluoracetic acid for *t*-butyl ester or lithium hydroxide for methyl ester afforded the linker-connected ATR inhibitors **12a-e** and **13a-f**.

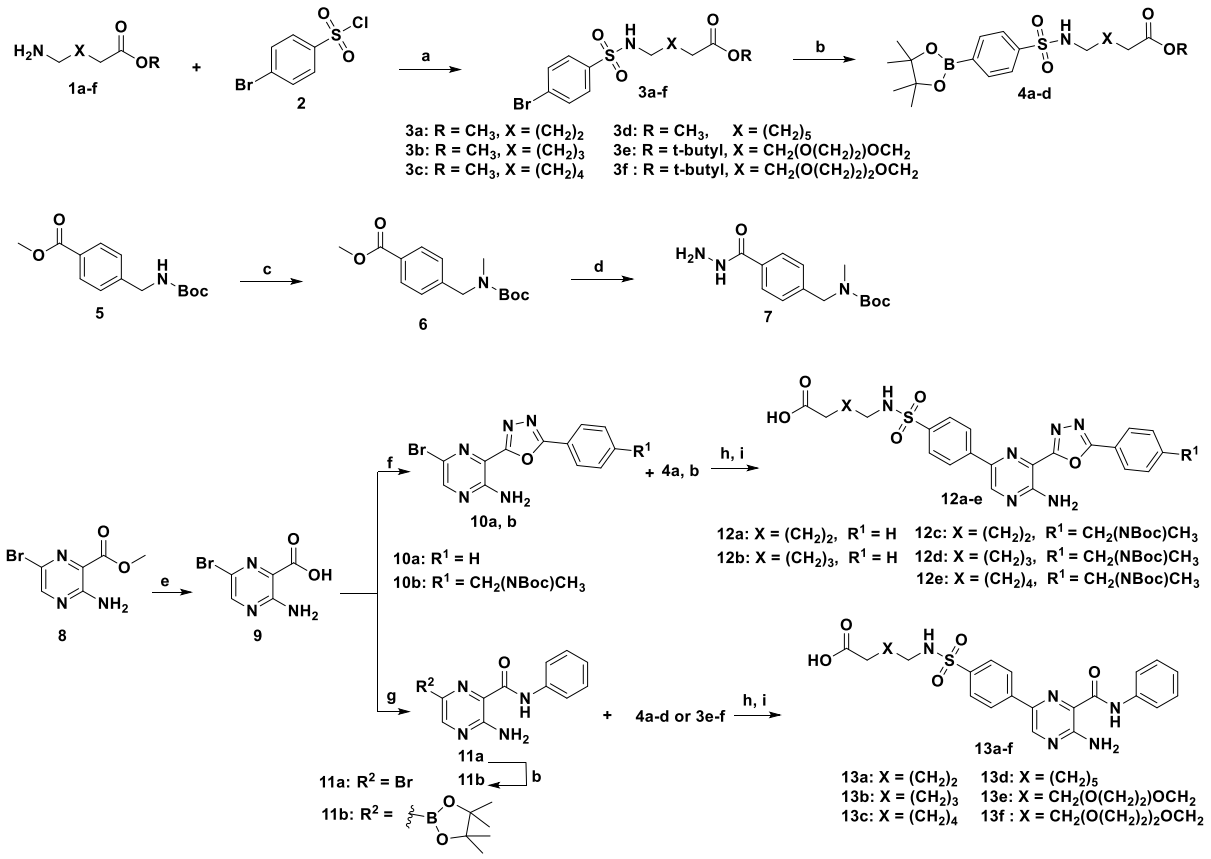

Scheme 1: Reagents and conditions: (a) TEA, Acetonitrile (b) B_2pin_2, Pd(dppf)Cl_2 KOAc, Dioxan (c) CH_3I, NaH, DMF (d) $NH_2NH_2.H_2O$, CH_3OH (e) LiOH, H_2O, CH_3OH (f) Benzohydrazides, PPh_3, CBr_4, TEA (g) Aniline, HATU, DIPEA, DMF (h) Pd(dppf)Cl_2 Na_2CO_3, Dioxan, H_2O (i) For methyl esters: LiOH, H_2O, THF. For t-butyl esters: DCM, TFA.

On the other hand, several cereblon warheads were prepared based on the structures of the reported cereblon ligands lenalidomide, thalidomide, and other glutarimides. The lenalidomide-based ligands were prepared as described in Scheme 2. First, a radical brominating reaction occurred between methyl 3-bromo-2-methyl benzoate **14** and NBS in the presence of benzoyl peroxide to give the corresponding 2-bromomethyl derivative **15,** which was further reacted with 3-aminopiperidine-2,6-dione **16** in the presence of triethylamine to yield the lenalidomide derivative **17a** [27, 28]. Then, the latter was methylated with methyl iodide using potassium carbonate as a base to give the corresponding *N*-methylated analog **17b** (which will be used for the negative control synthesis) [28]. Finally, intermediates **20a-c** were synthesized by Sonogashira coupling reactions between the compounds **17a, b** and terminal alkyne linkers **18a, b** followed by Boc-deprotection under acidic conditions [29].

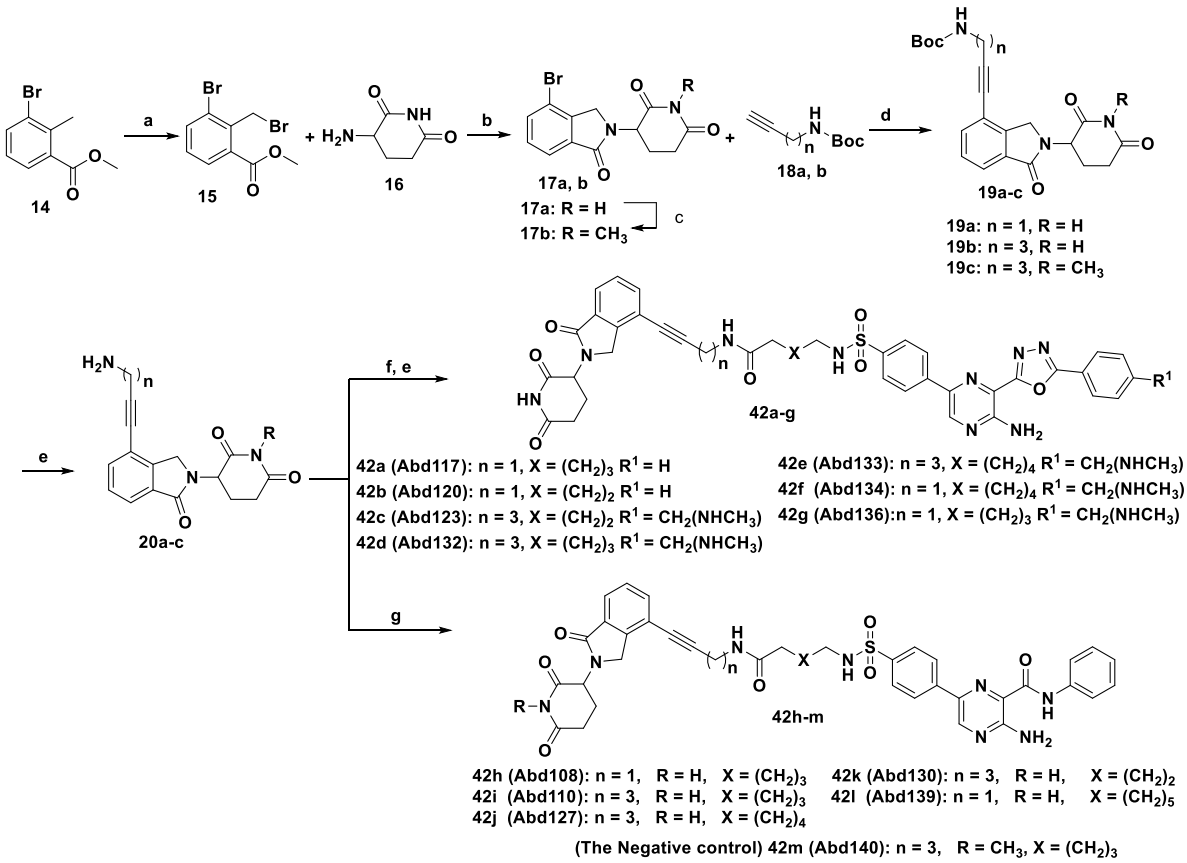

Scheme 2: Reagents and conditions: (a) NBS, BPO, CCl_4 (b) TEA, Acetonitrile (c) CH_3I, K_2CO_3, DMF (d) $Pd(dpp)_2Cl_2$ TEA, DMF (e) DCM, TFA (f) **12a-e**, HATU, DIPEA, DMF (g) **13a-f**, HATU, DIPEA, DMF

Also, the thalidomide-based cereblon ligand **25** was synthesized as shown in Scheme 3. The 4-fluorophthalic anhydride **21** was reacted with 3-aminopiperidine-2,6-dione **16** to afford the 5-flurothalidomide **22,** which was then converted to its piperazine analog **24** through its reaction with 1-Boc-piperazine **23,** followed by Boc-deprotection to afford the thalidomide analog **25** [28, 30]. In addition, the synthetic pathway for the phenyl-glutarimide derivative **28** was illustrated in Scheme 4. The 3-bromopyridine derivative **26** was coupled with 4-hydroxyphenyl boronic acid **27** using the Suzuki cross-coupling condition to afford the corresponding 3-phenylpyridine derivative **28** [31]. Then, the hydroxyl group of intermediate **28** was alkylated with *N*-Boc-2-bromoethylamine to produce the corresponding alkylated derivative **29**. Finally, a palladium-catalyzed hydrogenation reaction is used to remove the two benzyl groups and saturate the pyridine ring, followed by Boc-deprotection under acidic condition, affording the phenyl-glutarimide derivative **31** [31]. Furthermore, the picolinamide glutarimide derivative **35** was synthesized according to Scheme 4. The 6-fluoropicolinic acid **32** was coupled with 3-aminopiperidine-2,6-dione **16** to afford the 6-

fluoropicolinamide derivative **33,** which was then converted to its piperazine analog **34** through its reaction with 1-Boc-piperazine **23,** followed by Boc-deprotection to afford the picolinamide glutarimide derivative **35.**

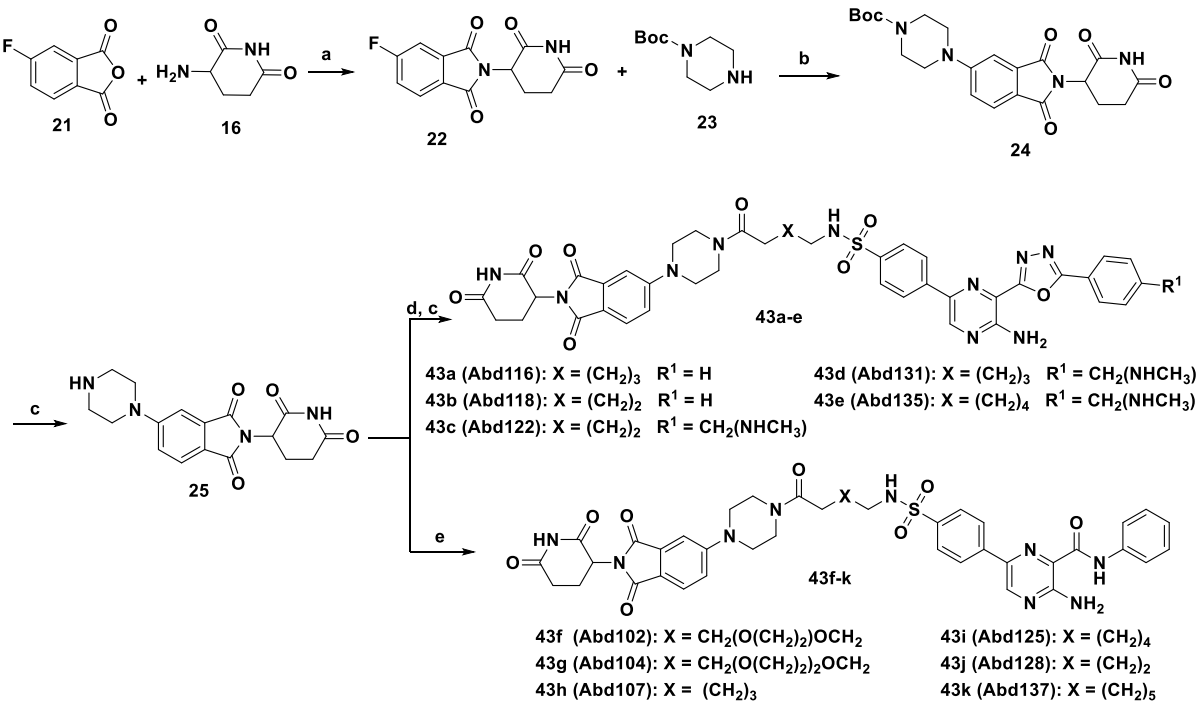

Scheme 3: Reagents and conditions: (a) AcOH, NaOAc (b) DIPEA, DMSO (c) DCM, TFA (d) **12a-e,** HATU, DIPEA, DMF (e) **13a-f**, HATU, DIPEA, DMF

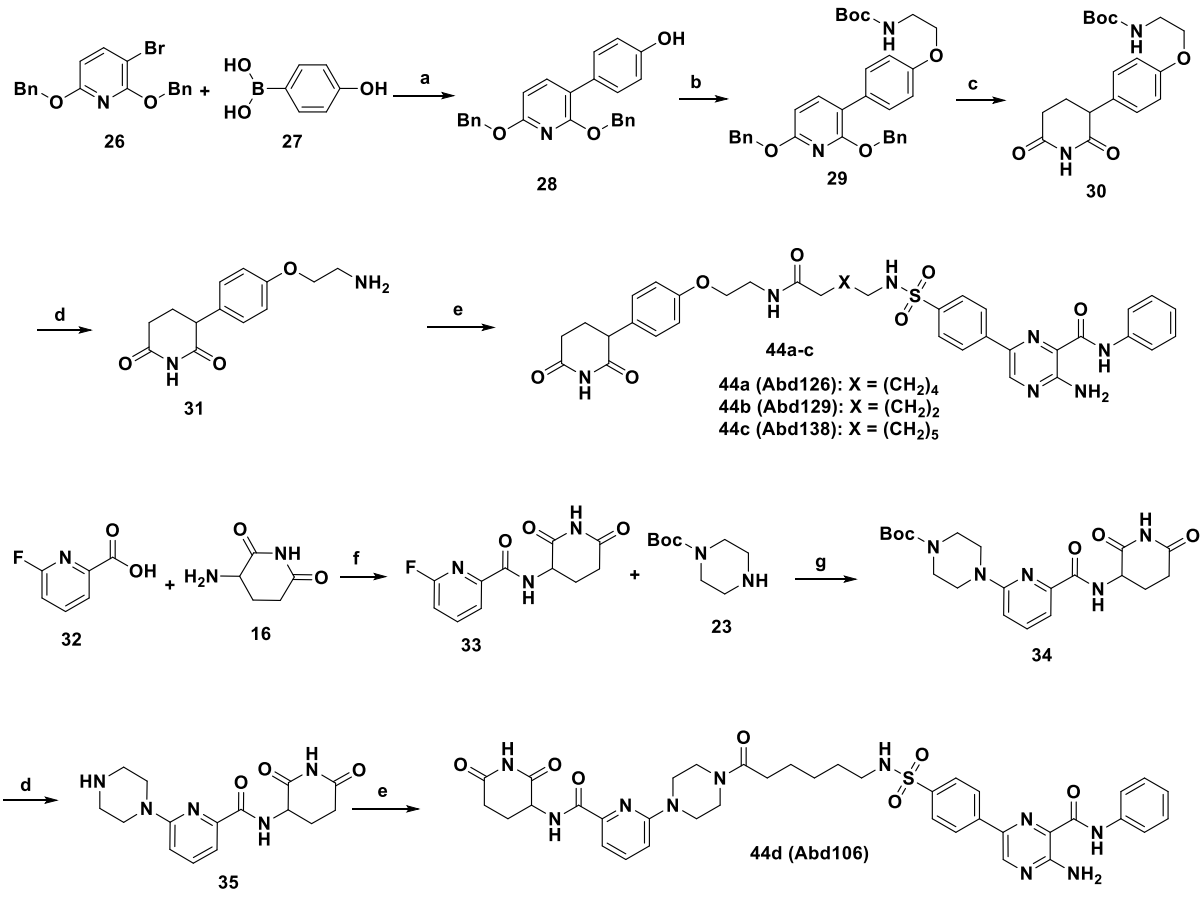

Scheme 4: Reagents and conditions: (a) $Pd(dppf)Cl_2$ Na_2CO_3, Dioxan, H_2O (b) Cs_2CO_3, *N*-Boc-2-bromoethyl amine (c) 10% Pd/C, THF(d) DCM, TFA (e) **13a-f,** HATU, DIPEA, DMF (f) thionyl chloride, Acetonitrile, TEA (g) DIPEA, DMSO

Finally, The VHL-based PROTACs were synthesized using the VHL ligand **41** which has prepared following the previously reported procedures, as illustrated in Scheme 5 [32]. The *N*-Boc-4-bromobenzyl amine **36** was coupled with 4-methylthiazole, using the Heck coupling reaction followed by Boc-deprotection to afford the intermediate **37.** Then, the intermediate **37** was coupled with *N*-Boc-L-hydroxyprolin **38** and *N*-Boc-L-*tert*-leucine **40** respectively, through a HATU-mediated coupling reaction followed by Boc-deprotection after each coupling reaction afforded the corresponding VHL building block **41**.

The structures of the synthesized VHL-PROTACS and CRBN-PROTACS are outlined in table 1 and table 2, respectively.

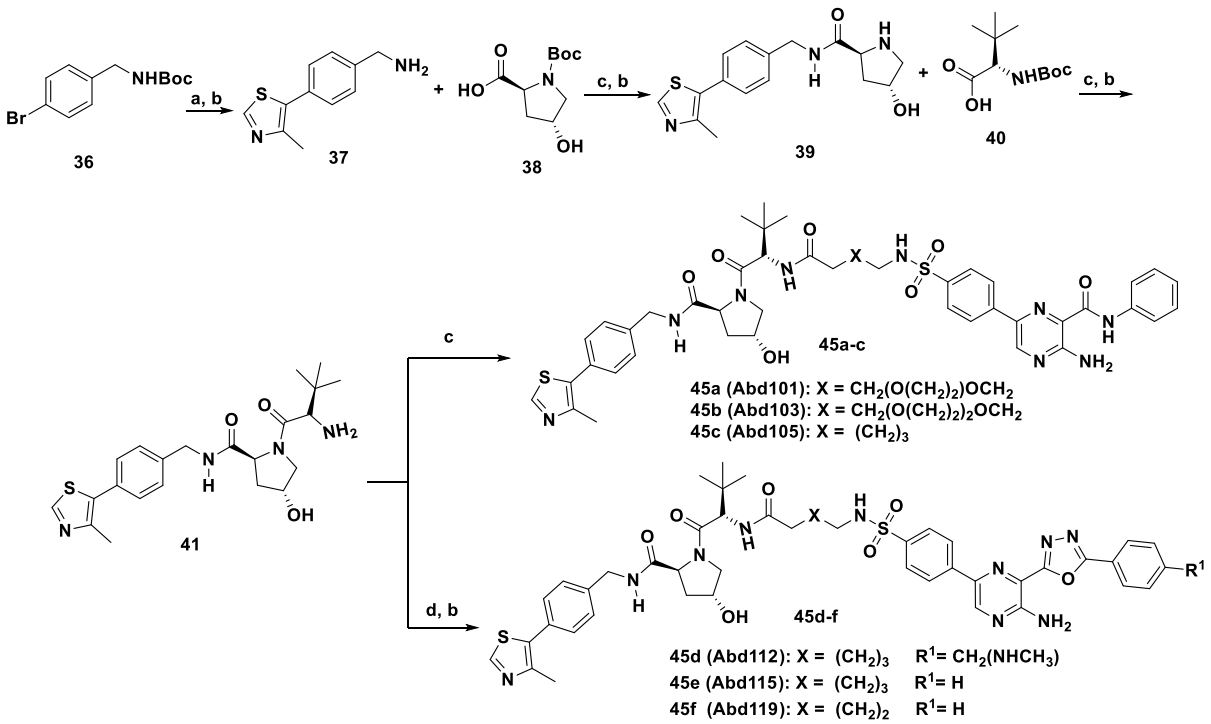

Scheme 5: Reagents and conditions: (a) 4-methylthiazole, $Pd(OAc)_2$, KOAc, DMF (b) DCM, TFA (c) **13a-f**, HATU, DIPEA, DMF (d) **12a-e**, HATU, DIPEA, DMF

Table 1: Chemical structures of developed VHL-based PROTACs

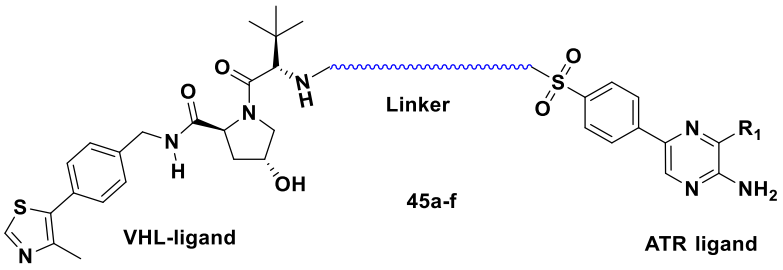

Cmpd. ID	Linker	R1
45a (Abd101)	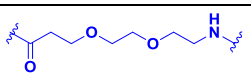	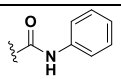
45b (Abd103)	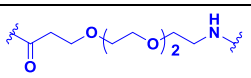	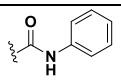
45c (Abd105)	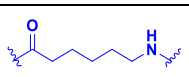	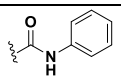
45d (Abd112)	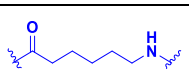	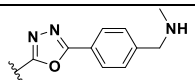
45e (Abd115)	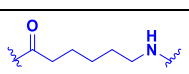	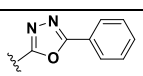
45f (Abd119)	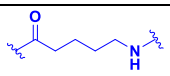	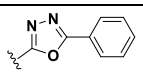

Table 2: Chemical structures of developed CRBN-based PROTACs

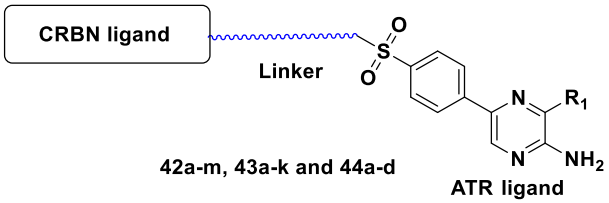

Cmpd. ID	CRBN ligand	Linker	R1
42a (Abd117)	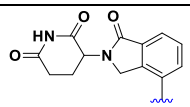	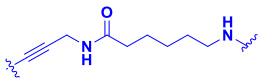	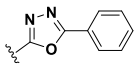
42b (Abd120)	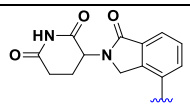	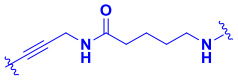	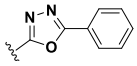
42c (Abd123)	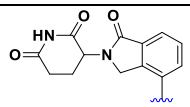	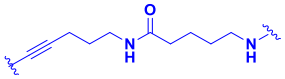	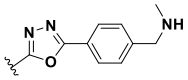
42d (Abd132)	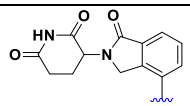	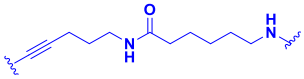	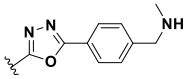
42e (Abd133)	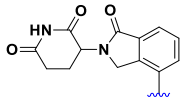	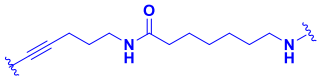	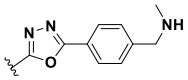
42f (Abd134)	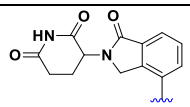	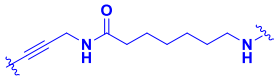	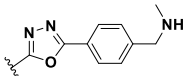
42g (Abd136)	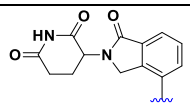	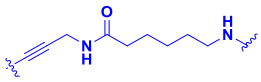	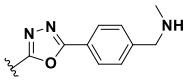
42h (Abd108)	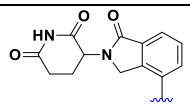	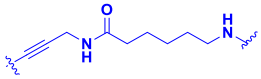	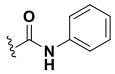
42i (Abd110)	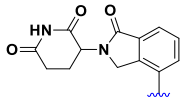	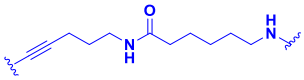	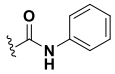
42j (Abd127)	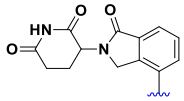	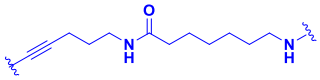	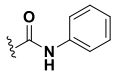
42k (Abd130)	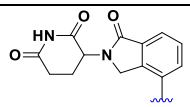	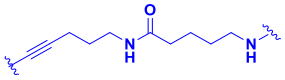	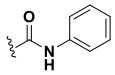
42l (Abd139)	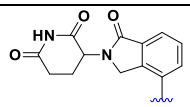	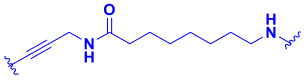	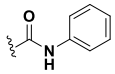

42m (Abd140) (negative control)	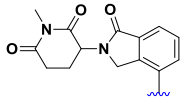	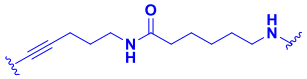	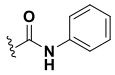
43a (Abd116)	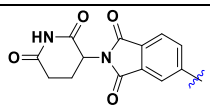	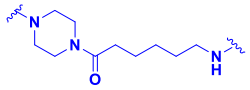	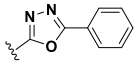
43b (Abd118)	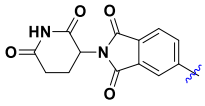	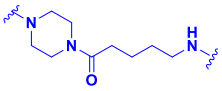	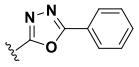
43c (Abd122)	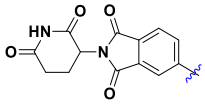	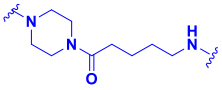	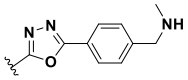
43d (Abd131)	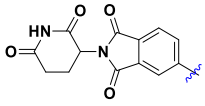	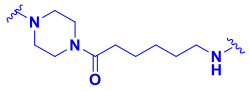	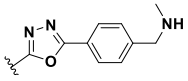
43e (Abd135)	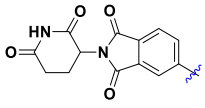	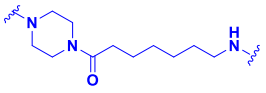	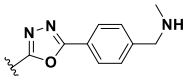
43f (Abd102)	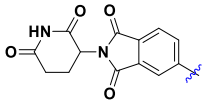	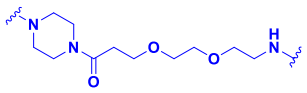	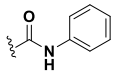
43g (Abd104)	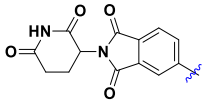	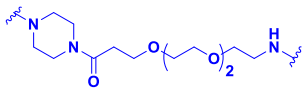	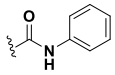
43h (Abd107)	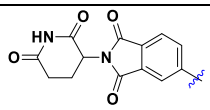	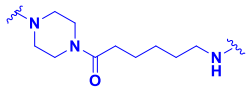	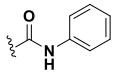
43i (Abd125)	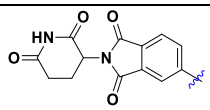	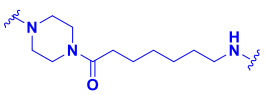	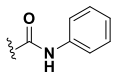
43j (Abd128)	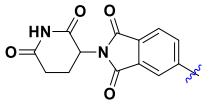	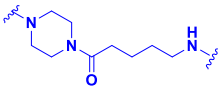	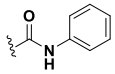
43k (Abd137)	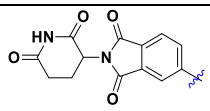	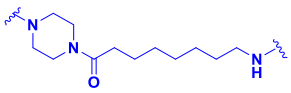	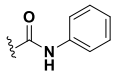
44a (Abd129)	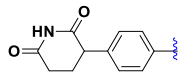	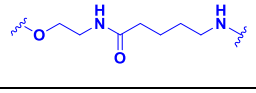	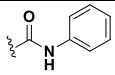
44b (Abd126)	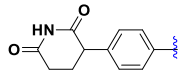		
44c (Abd138)			
44d (Abd106)			

2.1.1 Non-enzymatic stability testing for selected compounds.

The reported CRBN-based PROTACs usually depend on the cereblon ligand thalidomide and its structurally related imide drugs (IMiDs) which are inherently unstable and readily undergoing hydrolysis in body fluids [33]. Also, it was found that IMiDs and IMiD-based PROTACs rapidly hydrolyze in PBS, and in relatively mild and widely utilized cell media [31]. Therefore, we tested the chemical stability of our synthesized PROTACs under cellular assay condition, we used a non-enzymatic stability assay method. The selected CRBN-based PROTACs were dissolved in DMSO (10μM) then diluted in the cellular assay media (Dulbecco's modified Eagle medium (DMEM) (50%)/dimethyl sulfoxide (DMSO) (10%)/acetonitrile (40%)) and incubated at 37 °C for a maximum of 72 h. The HPLC was used to determine the quantity of the compounds after 6, 12, 24, 48, and 72 h intervals.

The results of the stability studies are presented in **Table 3.** It was founded that all tested compounds showed a relative stability at cellular assay conditions over 72 h except for compound **43f** (Abd102), which was only stable for 24h. Also, it was observed that lenalidomide and phenyl-glutarimide based PROTACs including the most active compound **42i** (Abd110) showed a higher chemical stability profile without any degradation product after 72h. While the thalidomide based PROTACs showed moderate stability and showed two degradation products after 72h.

Table 3: Stability of selected CRBN-based PROTACs in assay medium at 37 °C.

Cmpd. Id	**Stability %**					
	0 h	**6 h**	**12 h**	**24 h**	**48 h**	**72 h**
42b (Abd120)	100	104	104	105	103	107
42h (Abd108)	100	101	103	103	105	109
42i (Abd110)	100	102	104	106	110	115
42j (Abd127)	100	102	103	104	105	109
42k (Abd130)	100	102	102	102	103	103
43a (Abd116)	100	96	93	90	80	73
43b (Abd118)	100	99	95	91	85	77
43f (Abd102)	100	100	95	80	21	6
43g (Abd104)	100	101	100	97	83	74

43h (Abd107)	100	101	101	96	87	72
43i (Abd125)	100	97	92	88	78	70
43j (Abd128)	100	97	94	90	82	74
43k (Abd137)	100	98	105	108	94	84
44a (Abd126)	100	101	103	102	102	101
44b (Abd129)	100	101	101	101	99	99

2.2. Biological evaluation

2.2.1 ATR degradation

We commenced our experiment with the screening of VHL-based, putative PROTACs in cellulo. The treatment of pancreatic cancer cells MIA PaCa-2 (isolated from the carcinoma of a 65-year-old male) with different doses of the VHL-based PRTOACs **45a-c** (Abd101, Abd103, and Abd105) for 24 h yielded no reduction of ATR levels when compared to untreated cells. High doses (2 and 5 μM) of such PROTACs even increased ATR protein levels (Figure 4a). Therefore we did not test the remaining VHL-based PROTACs **45d-f** and focused on the testing of CRBN-based PROTACs. Lenalidomide (CRBN ligand)-based PROTACs could attenuate ATR expression. 500 nM of **42i** (Abd110) (based on the ATR inhibitor **VE-821**) reduced ATR to 40% of its levels in untreated cells. To study the optimal linker length, we tested **42j** (Abd127) and **42k** (Abd130). These compounds harbor longer or shorter linker lengths, respectively, than **42i** (Abd110). 1 μM **42j** (Abd127) produced similar ATR-reducing effects as **42i** (Abd110) but failed to attenuate the expression of ATR in its active form, i.e., phosphorylated at the T1989 residue. **42j** (Abd127) even augmented this posttranslational modification of ATR. **42k** (Abd130) was less active than **42i** (Abd110). Treatment with 2 μM **42h** (Abd108), which was also designed based on **VE-821**, could decrease ATR levels by 50%. **42l** (Abd139) proved to be less effective than such compounds (Figure 4b). We additionally tested lenalidomide-based PROTACs that contain VE-822 and **II** as ATR inhibitors. 40% reduction in ATR levels was achievable with 2 μM **42a** (Abd117) and **42c** (Abd123). Very weak effects on ATR expression levels (not exceeding 20% reduction) were observed with **42e-g** (Abd133, Abd134, and Abd136). Only a slight increase in ATR levels was noted with **42b** (Abd120) and **42d** (Abd132) (Figure 1c).

Different doses of the thalidomide- and **VE-821**-based PROTACs **43f** (Abd102)**, 43g** (Abd104)**, 43j** (Abd128)**,** and **43k** (Abd137) either had no effects on ATR levels or even raised its expression. Of such PROTACs, 5 μM **43h** (Abd107) reduced ATR to 40% of its

levels in untreated cells, but a minor lessening effect was noted upon **43i** (Abd125) treatment (Figure 4d). Considering the thalidomide-based PROTACs that harbor other ATR inhibitor moieties, weak attenuation of ATR expression was observed upon 24 h treatment of pancreatic cancer cells with **43b** (Abd118)**, 43c** (Abd122)**,** and **43e** (Abd135). Immunoblot analyses revealed that **43a** (Abd116) and **43d** (Abd131) induced higher ATR expression levels than those in control cells (Figure 4e). We expanded our study to include PROTACs based on other glutarimide moieties exemplified by **44a** (Abd126) and **44b** (Abd129), which could not reduce ATR levels reproducibly, as well as **44c** (Abd138) and **44d** (Abd106), which augmented the ATR protein levels (Figure 4f). Thus, our biological screening positions **42i** (Abd110) as the most promising compound.

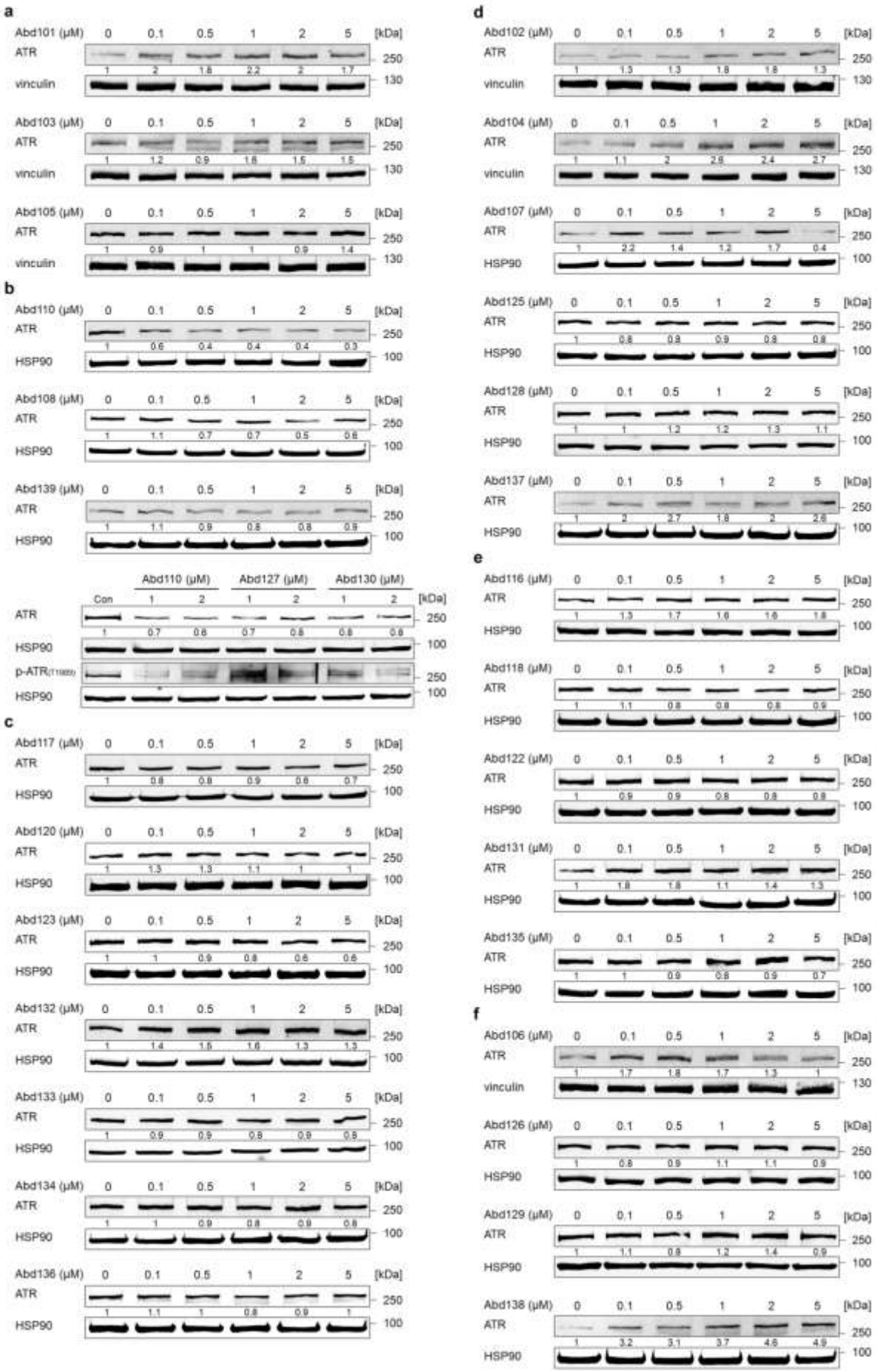

Figure 4. Screening of ATR-PROTACs in cancer cells. (a) Lysates from MIA PaCa-2 cells that were treated with the VHL-based PROTACs Abd101, Abd103, and Abd105 (0.1, 0.5, 1, 2, and 5 μM) for 24 h were subjected to immunoblot analyses. The immunoblots show ATR; vinculin serves as independent loading control for each membrane. (b) Lysates from MIA PaCa-2 cells that were treated with the lenalidomide- and VE-821-based PROTACs Abd110, Abd108, Abd139 (0.1, 0.5, 1, 2, and 5 μM), Abd127, and Abd130 (1 and 2 μM) for 24 h were subjected to immunoblot analyses. The immunoblots show ATR and p-ATR (T1989); HSP90 serves as independent loading control for each membrane. (c) Lysates from MIA PaCa-2 cells that were treated with the lenalidomide- and other ATR inhibitor-based PROTACs Abd117, Abd120, Abd123, Abd132, Abd133, Abd134, and Abd136 (0.1, 0.5, 1, 2, and 5 μM) for 24 h were subjected to immunoblot analyses. The immunoblots show ATR; HSP90 serves as independent loading control for each membrane. (d) Lysates from MIA PaCa-2 cells that were treated with the thalidomide- and VE-821-based PROTACs Abd102, Abd104, Abd107, Abd125, Abd128, and Abd137 (0.1, 0.5, 1, 2, and 5 μM) for 24 h were subjected to immunoblot analyses. The immunoblots show ATR; HSP90 and vinculin serve as independent loading controls for each membrane. (e) Lysates from MIA PaCa-2 cells that were treated with the thalidomide- and other ATR inhibitor-based PROTACs Abd116, Abd118, Abd122, Abd131, and Abd135 (0.1, 0.5, 1, 2, and 5 μM) for 24 h were subjected to immunoblot analyses. The immunoblots show ATR; HSP90 serves as independent loading control for each membrane. (f) Lysates from MIA PaCa-2 cells that were treated with other glutarimide-based PROTACs Abd106, Abd126, Abd129, and Abd138 (0.1, 0.5, 1, 2, and 5 μM) for 24 h were subjected to immunoblot analyses. The immunoblots show ATR; HSP90 and vinculin serve as independent loading controls for each membrane. Numbers below the respective proteins indicate densitometric values of the protein expression levels, normalized to the loading controls; protein levels of untreated cells were defined as 1.0 (n = 2 ± SD).

We pursued other experiments with **42i** (Abd110) as it was the most potent and dose-dependent ATR degrader in our screen. To investigate the effects of **42i** (Abd110) on ATR-related checkpoint kinases, we analyzed ATM and DNA-PKcs protein levels upon treatment of MIA PaCa-2 cells with different doses of **42i** (Abd110). The levels of these checkpoint kinases as well as the expression of the pro-proliferative CRBN neosubstrate GSPT1 did not change in **42i** (Abd110) treated cancer cells (Figure 5a). To verify our results in an independent cell system, we used cervix carcinoma cells (HeLa, from a 31-year-old female). In these cells, we noted a degradation of ATR and p-ATR by 60-70% upon treatment with 500 nM **42i** (Abd110). The ATR-related proteins ATM and DNA-PKcs were not attenuated by **42i** (Abd110) (Figure 5b). These data show that **42i** (Abd110) decreases ATR and p-ATR levels without affecting related apical checkpoint kinases in male and female tumor cells from different anatomical sites.

To verify the anticipated proteasomal ATR degradation, we pre-incubated MIA PaCa-2 cells with two structurally different proteasome inhibitors, bortezomib (50 nM) and MG132 (10 μM), and then treated the cells with 2 μM **42i** (Abd110) for 3 h. We chose this shorter time point to avoid the detection of processes that are related to proliferation arrest and cell death upon proteasome inhibition. Both inhibitors rescued the **42i** (Abd110) mediated ATR degradation (Figure 5c), verifying that **42i** (Abd110) accelerates the proteasomal degradation of ATR.

To corroborate that **42i** (Abd110) is an ATR degrader, we treated MIA PaCa-2 cells with the ATR inhibitor **VE-821** on which our PROTAC is based. **VE-821** failed to decrease ATR expression. Consistent with the above findings, **42i** (Abd110) significantly reduced ATR levels by 40% (Figure 5d). Hence, the ATR PROTAC **42i** (Abd110) has functional properties superseding its parental compound. To further corroborate the functionality of CRBN for the **42i** (Abd110) induced ATR degradation, we designed the **42i** (Abd110) derived negative control **42m** (Abd140). This molecule cannot bind CRBN due to methylated glutarimide moiety. **42m** (Abd140) failed to reduce ATR level as a single treatment of MIA PaCa-2 cells (Figure 5d).

Next, we asked if **42i** (Abd110) could reduce ATR that was activated upon DNA replication stress. Combinatorial treatment of cancer cells with the topoisomerase I inhibitor irinotecan (5 μM), which is used to treat PDAC [34], and **42i** (Abd110) attenuated the ATR levels by 80% relative to single chemotherapeutic treatment regimen. Irinotecan induced high expression levels of both p-ATR (T1989) and its direct downstream target p-CHK1 (S345). **42i** (Abd110) reduced their levels up to 0.1- and 0.5-fold, respectively (Figure 5e).

Due to its lenalidomide part, **42i** (Abd110) is expected to decrease ATR through a CRBN-containing E3 ubiquitin ligase complex. We aimed to prove this with a genetic approach using RNAi. A transient knock-down of CRBN consolidated the anticipated ATR degradation by **42i** (Abd110). Treatment of MIA PaCa-2 cells with siRNA against CRBN halted the PROTAC-mediated depletion of ATR, p-ATR, and p-CHK1 expression levels. Irinotecan and **42i** (Abd110) did not alter CRBN expression (Figure 5e).

2.2.2 Cytotoxicity of most promising compound against HEK239 cells

To test the potential toxicity of our most active ATR PROTAC on human embryonic kidney cell line (HEK293), we did cytotoxicity test with **42i** (Abd110). **42i** (Abd110) did not produce cytotoxic effects against HEK293 cells at a high concentration (50 μM) after 24h.

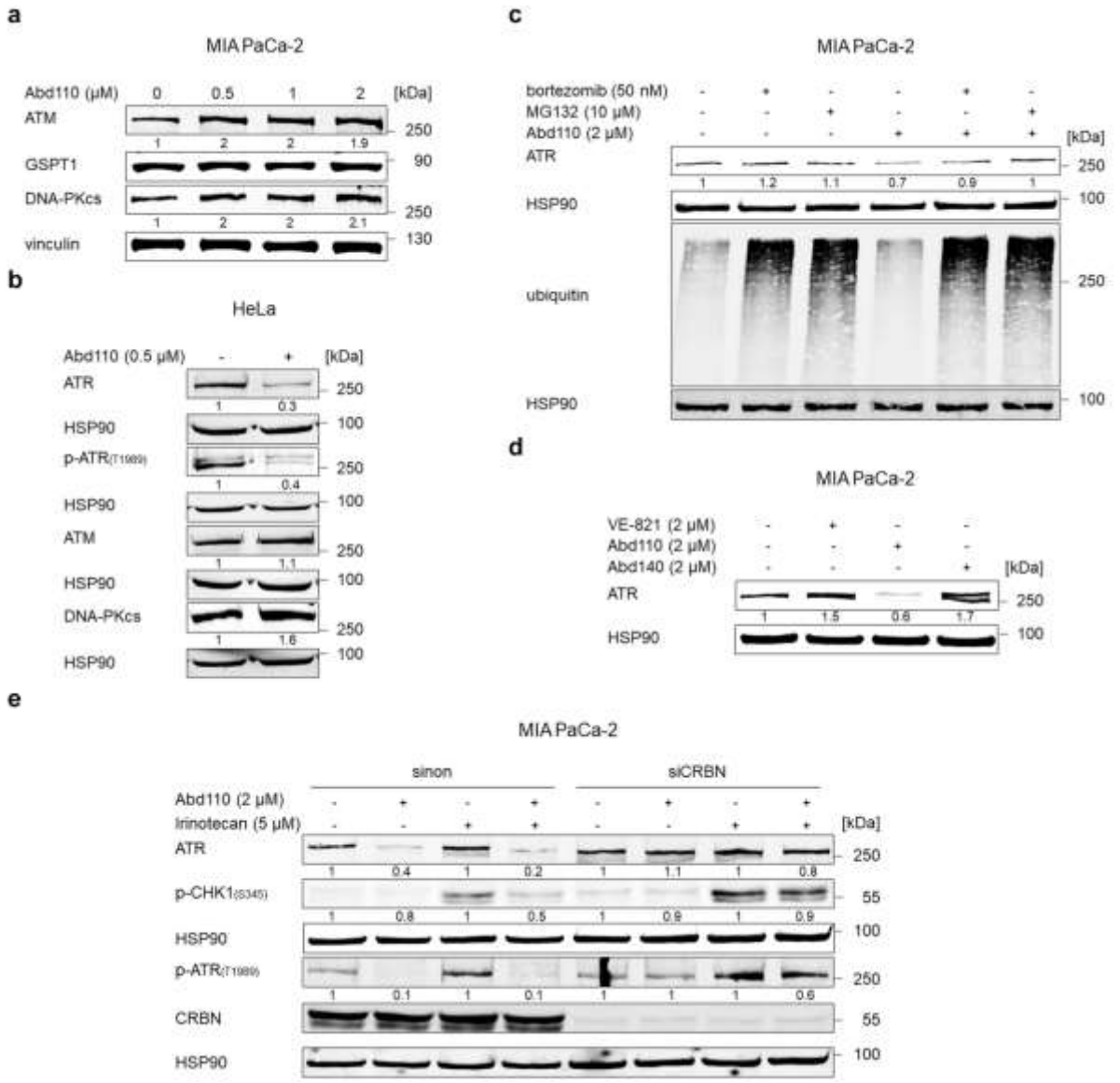

Figure 5. Specificity of the ATR-PROTAC **Abd110** in cancer cells. (a) Lysates from MIA PaCa-2 cells that were treated with **Abd110** (0.5, 1, and 2 μM) for 24 h were subjected to immunoblot analyses. The immunoblots show ATM, GSPT1, and DNA-PKcs; vinculin serves as independent loading control for each membrane. (b) Lysates from HeLa cells that were treated with **Abd110** (0.5 μM) for 24 h were subjected to immunoblot analyses. The immunoblots show ATR, p-ATR (T1989), ATM, and DNA-PKcs. HSP90 serves as loading control for each membrane. (c) Lysates from MIA PaCa-2 cells that were treated with **Abd110** (2 μM) for 3 h and/or bortezomib (50 nM) or **MG132** (10 μM) for 4 h were subjected to immunoblot analyses. The immunoblots show ATR and ubiquitin; HSP90 serves as independent loading control for each membrane. (d) Lysates from MIA PaCa-2 cells that were treated with the ATR inhibitor **VE-821** (2 μM), **Abd110** (2 μM), and **Abd140** (2 μM) for 24 h were subjected to immunoblot analysis. The immunoblot shows ATR; HSP90 serves as loading control for the membrane. (e) Lysates from MIA PaCa-2 cells (with and without CRBN knockdown by RNAi) that were treated with **Abd110** (2 μM) and/or irinotecan (5 μM) for 24 h. The immunoblots show ATR, p-CHK1 (S345), p-ATR (T1989), and CRBN; HSP90 serves as independent loading control for each membrane; siNon, non-targeting

control siRNA. Numbers below the respective proteins indicate densitometric values of the protein expression levels, normalized to the loading controls; protein levels of untreated and single irinotecan-treated cells were defined as 1.0 (n = 2 ± SD).

3. Conclusion

We presented the first-in-class ATR-targeting PROTACs based on three potent and selective ATR inhibitors containing a 3-aminopyrazine scaffold. The lenalidomide (CRBN ligand)-based PROTAC **42i** (Abd110) exhibits the highest ATR degradation potential of the synthesized agents that we tested in the pancreatic cancer cell line MIA PaCa-2. **42i** (Abd110) selectively decreases ATR and phospho-ATR without affecting the related apical checkpoint kinases ATM and DNA-PKcs. In addition, both proteasome inhibitors (MG-132 and bortezomib) as well as knock-down of CRBN prevent the **42i** (Abd110) mediated depletion of ATR, emphasizing that **42i** (Abd110) induces ATR degradation through the ubiquitin-proteasome-system. In addition, **42i** (Abd110) attenuates the activated ATR signalling pathway efficiently in cells with replication stress. In summary, these results suggest that **42i** (Abd110) is a promising candidate for further optimization and biological characterization as inducers of ATR degradation through proteasomes.

4. EXPERIMENTAL SECTION

4.1. General.

All materials and reagents were purchased from Sigma Aldrich Co. Ltd. and abcr GmbH and used without further purification. All solvents were analytically pure and were dried before use. All reactions were monitored by TLC (Kieselgel 60 F254 pre-coated plates, E. Merck, Darmstadt, Germany); the spots were detected by UV lamp at λ 254nm. For medium-pressure liquid chromatography (MPLC), Biotage SNAP ultra-HP-sphere 25μm columns containing silica gel were used. Dichloromethane: methanol and n-heptane: Ethyl acetate were used as elution systems for MPLC. In the preparative high-pressure liquid chromatography used for purification of several PROTACs, LiChrosorb® RP-18 (7 μm) 250-25 Merck (Merck, Darmstadt, Germany) column was used. The applied mobile phase was a gradient with increasing polarity composed of acetonitrile/water/formic acid. Purity was determined using HPLC by measuring the UV absorbance at 254 nm. The HPLC consisted of a LiChrosorb® RP-18 (5 μm) 100-4.6 Merck column (Merck, Darmstadt, Germany), two LC-10AD pumps, a SPD-M10A VP PDA detector, and a SIL-HT autosampler, all from the

manufacturer Shimadzu (Kyoto, Japan). The absorption spectra were recorded with a SPD-M10A diode array detector Shimadzu spectrophotometer (Kyoto, Japan). Mass spectrometry analyses were performed with a Finnigan MAT710C (Thermo Separation Products, SanJose, CA, USA) for the ESI MS spectra and with a LTQ (linear ion trap) Orbitrap XL hybrid mass spectrometer (Thermo Fisher Scientific, Bremen, Germany) for the HRMS-ESI (high-resolution mass spectrometry) spectra. ^{1}HNMR and ^{13}CNMR spectra were taken on a Varian Inova 400 using deuterated dimethyl sulfoxide (DMSO-d_6) or deuterated chloroform ($CDCl_3$) as solvent. Chemical shifts were referenced to the residual solvent signals. The following abbreviations and formulas for solvents and reagents were used: ethyl acetate (EtOAc), N,N-dimethylformamide (DMF), dimethyl sulfoxide (DMSO), tetrahydrofuran (THF), triethylamine (TEA), water (H_2O), dichloromethane (DCM), N,N-diisopropylethylamine (DIPEA), O-(7-azabenzotriazol-1-yl)-*N*,*N*,*N*′,*N*′-tetramethyluronium-hexafluorphosphate (HATU), Triphenylphosphine (PPh_3), bis(pinacolato)diboron (B_2pin_2), (1,1'-Bis(diphenylphosphino)ferrocene)palladium(II) dichloride ($Pd(dppf)Cl_2$) and trifluoroacetic acid (TFA).

4.2. General Synthetic Methods.

Method I: Reaction of amine and acid chloride

To a stirred solution of the appropriate amine (1.0 equiv.) and triethylamine (3 equiv.) in acetonitrile at 0 $^{\circ}$C, acid chloride (1.05 equiv.) was added. Then, the reaction mixture was allowed to stir at room temperature for 4-7 hours. After completion of the reaction as indicated by TLC, the reaction was quenched with 5% acetic acid solution and extracted with ethyl acetate. The combined organic layer was washed with brine and dried over anhydrous sodium sulfate, then the solvent was evaporated under reduced pressure to yield the crude amide, which was purified by the MPLC using n-heptane/ethyl acetate or MeOH/DCM.

Method II: Hydrolysis of methyl ester.

To a stirred solution of the appropriate methyl ester (1.0 equiv.) in THF:H_2O (3:1), $LiOH.H_2O$ (5.0 equiv.) was added, and the mixture was stirred at room temperature for 4-6 hours. After complete ester hydrolysis, 1 M hydrochloric acid solution was added drop wise to the reaction to liberate the free acid, which was extracted with ethyl acetate. The combined organic layer was washed with brine and dried over anhydrous sodium sulfate, and then the solvent was evaporated under reduced pressure to give the corresponding carboxylic acid.

Method III: Hydrolysis of tert-butyl ester.

The appropriate *tert*-butyl ester was dissolved or suspended in DCM at 0 °C (5 mL), and then trifluoroacetic acid (5 mL) was added drop wise. The reaction mixture was stirred at room temperature for 3-4 hours. After complete ester hydrolysis, the solvent was evaporated to dryness to provide the corresponding carboxylic acid.

Method IV: Amide coupling.

A solution of the appropriate carboxylic acid (1.0 equiv.) and HATU (1.1 equiv.) in DMF was stirred at room temperature for 30 min., then the corresponding amine derivative (1.0 equiv.) and DIPEA (4.0 equiv.) were added. The reaction mixture was stirred at room temperature for 4–6 hours. After completion of the reaction as indicated by TLC, the reaction was quenched with 1 M ammonium chloride solution and extracted with ethyl acetate. The organic layer was washed with an aqueous 1 M sodium bicarbonate solution and brine. The combined organic layer was dried over anhydrous sodium sulfate, and then the solvent was evaporated under reduced pressure to yield the crude amide, which was purified by the MPLC using n-heptane/ethyl acetate or MeOH/DCM.

Method V: **Miyaura borylation**

A solution of bromoaryl derivative (1 equiv.), bis(pinacolato)diboron (1.2 equiv.), potassium acetate (3 equiv.), and Pd(dppf)Cl_2 (0.1 equiv.) in dioxan was degassed and flushed with argon three times, and then heated at 80 °C for 6-8 hours. The reaction mixture was cooled to room temperature, diluted with ethyl acetate, and filtered through celite. The filtrate was evaporated under reduced pressure to yield the crude product, which was purified by the MPLC using n-heptane/ethyl acetate or MeOH/DCM.

***Method VI: Suzuki coupling*.**

A solution of bromoaryl derivative (1 equiv.), the appropriate boronic derivative (1 equiv.), Na_2CO_3 (4 equiv.), and Pd(dppf)Cl_2 (0.1 equiv.) in 25 ml dioxan:H_2O (5:1) was degassed and purged with argon three times. The reaction mixture was heated at 90 °C for 6-8 hours. The reaction mixture was cooled to room temperature, diluted with ethyl acetate, and filtered through celite. The filtrate was evaporated under reduced pressure, and the residue was purified by MPLC using n-heptane/ethyl acetate.

Method VII: Boc-deprotection

Method VII-A: To a stirred solution or suspension of Boc-protected amine in DCM (5 mL) at 0 °C, trifluoroacetic acid (5 mL) was added drop wise, and the solution was stirred at room temperature for 1 hour. After completion of the reaction, the mixture was evaporated under reduced pressure to afford the crude product as trifluoroacetate salt, which can be directly used in the next step without further purification.

Method VII-B: To a stirred solution of Boc-protected amine and 1,2-ethanedithiol (0.5 mL) in DCM (5 mL) at 0 °C, trifluoroacetic acid (5 mL) was added drop wise and the solution was stirred at room temperature for 1 hour. After completion of the reaction, the mixture was evaporated under reduced pressure. After that, the residue was dissolved again in DCM, neutralized with triethyl amine and evaporated under reduced pressure to yield the crude product, which was purified by the MPLC or preparative HPLC.

Method VIII: Alkylation reaction

To a stirred solution of compound (**5, 17a** or **28** (1.0 equiv.)) and a base (K_2CO_3, Cs_2CO_3 or NaH (2.5 equiv.)) in 25 ml of DMF, an appropriate alkyl halide (2 equiv.) was added, and the solution was stirred at room temperature overnight. The mixture was diluted with 60 mL of water and extracted with ethyl acetate three times. The combined organic layers were washed with brine, dried over Na_2SO_4, and evaporated under reduced pressure to yield the crude product, which was purified by the MPLC using n-heptane/ethyl acetate or MeOH/DCM.

Method IX: Hydrogenation

To a stirred solution of compound **29** in THF (20 mL), a catalytic amount of Pd/C (10%) was added under an inert atmosphere, then the reaction mixture was stirred overnight under a hydrogen atmosphere at room temperature. The reaction mixture was filtered through a short pad of celite, washed with ethyl acetate and concentrated to dryness. The crude product was purified by the MPLC using n-heptane/ethyl acetate.

Method X: Synthesis of 1,3,4-Oxadiazole.

To a stirred mixture of pyrazine carboxylic acid **9** (1.0 equiv.), the appropriate benzohydrazide derivative (1.0 equiv.), tetrabromoethane (2.5 equiv.) and TEA (3.0 equiv.) in DCM (25 mL) at 0 °C, triphenylphosphine (2.5 equiv.) was added portion wise over ten

minutes, and the reaction was then stirred at room temperature for 2 hours. After that the mixture was evaporated under reduced pressure and the residue was purified by MPLC using n-heptane/ethyl acetate.

Method XI: Reaction of piperazine with fluoroaromatic compounds.

To a stirred solution of fluoroaromatic compound (1.0 equiv.) and DIPEA (3.0 equiv.) in DMSO (25 mL), 1-Boc-piperazine (1.1 equiv.) was added and the reaction was then heated at 130 °C for 4-5 hours. After completion of the reaction, the reaction was quenched with 5% acetic acid solution and extracted with ethyl acetate. The combined organic layer was washed with brine and dried over anhydrous sodium sulfate, then the solvent was evaporated under reduced pressure to yield the crude product, which was purified by the MPLC using n-heptane/ethyl acetate.

4.3. Characterization Data of Key Intermediates and Final Compounds.

The preparation and analytical data of Intermediates **9**, **11a** [8], **20a-c** [29], **25** [30], **28** [31] and **41** [32] were as reported.

4.3.1 Synthesis and characterization of intermediates 3a-f and 4a-d.

The 4-bromobenzensulfonyl chloride reacted with alkyl and PEG linkers **1a-f** according to method I to give the corresponding 4-bromobenzenesulphonamide derivatives **3a-f**. Then the intermediates **3a-d** were further converted to the corresponding boronates **4a-d** according to method V.

Methyl 5-((4-bromophenyl)sulfonamido)pentanoate (3a). ^{1}H NMR (400 MHz, $CDCl_3$) δ 7.74 – 7.68 (m, 2H), 7.66 – 7.61 (m, 2H), 5.04 (t, *J* = 6.0 Hz, 1H), 3.63 (s, 3H), 2.93 (q, *J* = 6.6 Hz, 2H), 2.26 (t, *J* = 7.1 Hz, 2H), 1.65 – 1.44 (m, 4H).

Methyl 6-((4-bromophenyl)sulfonamido)hexanoate (3b). ^{1}H NMR (400 MHz, $CDCl_3$) δ 7.74 – 7.69 (m, 2H), 7.66 – 7.61 (m, 2H), 4.91 (t, *J* = 6.1 Hz, 1H), 3.64 (s, 3H), 2.93 (dd, *J* = 13.3, 6.9 Hz, 2H), 2.25 (t, *J* = 7.4 Hz, 2H), 1.61 – 1.41 (m, 4H), 1.35 – 1.22 (m, 2H).

Methyl 7-((4-bromophenyl)sulfonamido)heptanoate (3c). ^{1}H NMR (400 MHz, $CDCl_3$) δ 7.74 – 7.69 (m, 2H), 7.67 – 7.61 (m, 2H), 4.86 (t, *J* = 5.1 Hz, 1H), 3.64 (s, 3H), 2.92 (dd, *J* = 13.3, 6.9 Hz, 2H), 2.26 (t, *J* = 7.4 Hz, 2H), 1.60 – 1.40 (m, 4H), 1.33 – 1.17 (m, 4H).

Methyl 8-((4-bromophenyl)sulfonamido)octanoate (3d). ^{1}H NMR (400 MHz, $CDCl_3$) δ 7.75 – 7.68 (m, 2H), 7.66 – 7.60 (m, 2H), 4.93 (t, *J* = 5.8 Hz, 1H), 3.64 (s, 3H), 2.91 (dd, *J* = 13.3, 6.9 Hz, 2H), 2.26 (t, *J* = 7.5 Hz, 2H), 1.62 – 1.37 (m, 4H), 1.30 – 1.15 (m, 6H).

Tert-butyl 3-(2-(2-((4-bromophenyl)sulfonamido)ethoxy)ethoxy)propanoate (3e). ^{1}H NMR (400 MHz, $CDCl_3$) δ 7.77 – 7.69 (m, 2H), 7.67 – 7.59 (m, 2H), 5.45 (t, *J* = 5.7 Hz, 1H), 3.69 (t, *J* = 6.3 Hz, 2H), 3.59 – 3.41 (m, 6H), 3.11 (dd, *J* = 10.4, 5.5 Hz, 2H), 2.49 (t, *J* = 6.4 Hz, 2H), 1.43 (s, 9H).

Tert-butyl 3-(2-(2-(2-((4-bromophenyl)sulfonamido)ethoxy)ethoxy)ethoxy)propanoate (3f). ^{1}H NMR (400 MHz, $CDCl_3$) δ 7.77 – 7.68 (m, 2H), 7.67 – 7.58 (m, 2H), 5.48 (t, *J* = 5.8 Hz, 1H), 3.69 (t, *J* = 6.5 Hz, 2H), 3.64 – 3.43 (m, 10H), 3.11 (dd, *J* = 10.4, 5.7 Hz, 2H), 2.48 (t, *J* = 6.5 Hz, 2H), 1.42 (s, 9H).

Methyl 5-((4-(4,4,5,5-tetramethyl-1,3,2-dioxaborolan-2-yl)phenyl)sulfonamido)pentanoate (4a). *m*/*z* (APCI$^+$) 398.2 (M+H). ^{1}H NMR (400 MHz, $CDCl_3$) δ 7.92 (d, *J* = 8.3 Hz, 2H), 7.82 (d, *J* = 8.3 Hz, 2H), 4.78 (t, *J* = 6.2 Hz, 1H), 3.62 (s, 3H), 2.92 (q, *J* = 6.7 Hz, 2H), 2.25 (t, *J* = 7.1 Hz, 2H), 1.64 – 1.43 (m, 4H), 1.34 (s, 12H).

Methyl 6-((4-(4,4,5,5-tetramethyl-1,3,2-dioxaborolan-2-yl)phenyl)sulfonamido)hexanoate (4b). *m*/*z* (APCI$^+$) 412.3 (M+H). ^{1}H NMR (400 MHz, $CDCl_3$) δ 7.92 (d, *J* = 8.3 Hz, 2H), 7.83 (d, *J* = 8.3 Hz, 2H), 4.67 (t, *J* = 6.2 Hz, 1H), 3.64 (s, 3H), 2.92 (dd, *J* = 13.4, 6.9 Hz, 2H), 2.24 (t, *J* = 7.4 Hz, 2H), 1.60 – 1.40 (m, 4H), 1.34 (s, 12H), 1.32 – 1.24 (m, 2H).

Methyl 7-((4-(4,4,5,5-tetramethyl-1,3,2-dioxaborolan-2-yl)phenyl)sulfonamido)heptanoate (4c). *m*/*z* (APCI$^+$) 426.3 (M+H). ^{1}H NMR (400 MHz, $CDCl_3$) δ 7.92 (d, *J* = 8.3 Hz, 2H), 7.83 (d, *J* = 8.3 Hz, 2H), 4.65 (t, *J* = 6.0 Hz, 1H), 3.64 (s, 3H), 2.91 (dd, *J* = 13.4, 6.8 Hz, 2H), 2.25 (t, *J* = 7.4 Hz, 2H), 1.58 – 1.40 (m, 4H), 1.34 (s, 12H), 1.29 – 1.22 (m, 4H).

Methyl 8-((4-(4,4,5,5-tetramethyl-1,3,2-dioxaborolan-2-yl)phenyl)sulfonamido)octanoate (4d). ^{1}H NMR (400 MHz, $CDCl_3$) δ 7.92 (d, *J* = 8.4 Hz, 2H), 7.83 (d, *J* = 8.4 Hz, 2H), 4.62 (t, *J* = 6.1 Hz, 1H), 3.64 (s, 3H), 2.91 (dd, *J* = 13.4, 6.9 Hz, 2H), 2.26 (t, *J* = 7.5 Hz, 2H), 1.60 – 1.37 (m, 4H), 1.34 (s, 12H), 1.27 – 1.15 (m, 6H).

4.3.2 Synthesis and characterization of intermediates 6 and 7

Compound **5** was methylated with methyl iodide to produce the corresponding intermediate **6** according to method VIII, which was then refluxed with hydrazine hydrate (10 equiv.) in methanol for overnight. After that, the solvent was evaporated under reduced pressure and the residue was purified by MPLC to afford the corresponding benzohydrazide derivative **7**.

Methyl 4-(((tert-butoxycarbonyl)(methyl)amino)methyl)benzoate (6). ^{1}H NMR (400 MHz, $CDCl_3$) δ 7.99 (d, *J* = 8.2 Hz, 2H), 7.27 (d, *J* = 7.8 Hz, 2H), 4.45 (s, 2H), 3.89 (s, 3H), 2.97 – 2.65 (m, 3H), 1.60 – 1.33 (m, 9H).

Tert-butyl (4-(hydrazinecarbonyl)benzyl)(methyl)carbamate (7). ^{1}H NMR (400 MHz, DMSO-d_6) δ 9.70 (s, 1H), 7.78 (d, *J* = 8.1 Hz, 2H), 7.25 (d, *J* = 8.2 Hz, 2H), 4.45 (s, 2H), 4.38 (s, 2H), 2.75 (s, 3H), 1.49 – 1.23 (m, 9H).

4.3.3 Synthesis and characterization of intermediates 10a, b

The pyrazine carboxylic acid **9** was reacted with the appropriate benzohydrazide derivative according to method X to obtain the corresponding 1,3,4-oxadiazole derivatives ***10a, b***.

5-Bromo-3-(5-phenyl-1,3,4-oxadiazol-2-yl)pyrazin-2-amine (10a). ^{1}H NMR (400 MHz, DMSO-d_6) δ 8.40 (s, 1H), 8.07 (dd, *J* = 8.0, 1.5 Hz, 2H), 7.75 (br, 2H), 7.69 – 7.56 (m, 3H).

Tert-butyl (4-(5-(3-amino-6-bromopyrazin-2-yl)-1,3,4-oxadiazol-2-yl)benzyl)(methyl)-carbamate (10b). ^{1}H NMR (400 MHz, DMSO-d_6) δ 8.40 (s, 1H), 8.07 (d, *J* = 8.1 Hz, 2H), 7.76 (br, 2H), 7.45 (d, *J* = 8.1 Hz, 2H), 4.46 (s, 2H), 2.80 (s, 3H), 1.53 – 1.23 (m, 9H).

4.3.4 Synthesis and characterization of intermediate 11b

The bromopyrazine derivative **11a** was converted to the corresponding pinacol boronic ester **11b** according to method V.

3-Amino-*N*-phenyl-6-(4,4,5,5-tetramethyl-1,3,2-dioxaborolan-2-yl)pyrazine-2-carboxamide (11b). *m/z* (APCI$^+$) 341.0 (M+H). ^{1}H NMR (400 MHz, DMSO-d_6) δ 10.15 (s, 1H), 8.42 (s, 1H), 7.81 (br, 2H), 7.72 (d, *J* = 7.7 Hz, 2H), 7.36 (t, *J* = 7.9 Hz, 2H), 7.12 (t, *J* = 7.4 Hz, 1H), 1.30 (s, 12H).

4.3.5 Synthesis and characterization of intermediates 12a-e and 13a-d

Pyrazine derivatives **10a, 10b** and **11a** were coupled with the appropriate boronic esters **4a-d** according to method VI, followed by ester hydrolysis according to method II to obtain the corresponding acids **12a-e** and **13a-d**.

5-((4-(5-Amino-6-(5-phenyl-1,3,4-oxadiazol-2-yl)pyrazin-2-yl)phenyl)sulfonamido) pentanoic acid (12a). ^{1}H NMR (400 MHz, DMSO-d_6) δ 11.96 (s, 1H), 8.99 (s, 1H), 8.29 (d, *J* = 8.5 Hz, 2H), 8.15 (dd, *J* = 7.6, 1.6 Hz, 2H), 7.88 (d, *J* = 8.5 Hz, 2H), 7.83 (br, 2H), 7.72 – 7.57 (m, 4H), 2.76 (dd, *J* = 12.6, 6.4 Hz, 2H), 2.14 (t, *J* = 7.0 Hz, 2H), 1.55 – 1.31 (m, 4H).

6-((4-(5-Amino-6-(5-phenyl-1,3,4-oxadiazol-2-yl)pyrazin-2-yl)phenyl)sulfonamido) hexanoic acid (12b). ^{1}H NMR (400 MHz, DMSO-d_6) δ 11.95 (s, 1H), 8.99 (s, 1H), 8.29 (d, *J* = 8.6 Hz, 2H), 8.16 (dd, *J* = 7.8, 1.7 Hz, 2H), 7.89 (d, *J* = 8.6 Hz, 2H), 7.82 (br, 2H), 7.71 – 7.57 (m, 4H), 2.75 (dd, *J* = 13.0, 6.8 Hz, 2H), 2.12 (t, *J* = 7.3 Hz, 2H), 1.47 – 1.31 (m, 4H), 1.28 – 1.13 (m, 2H).

5-((4-(5-Amino-6-(5-(4-(((tert-butoxycarbonyl)(methyl)amino)methyl)phenyl)-1,3,4-oxadiazol-2-yl)pyrazin-2-yl)phenyl)sulfonamido)pentanoic acid (12c). ^{1}H NMR (400 MHz, DMSO-d_6) δ 11.96 (s, 1H), 8.99 (s, 1H), 8.30 (d, *J* = 8.6 Hz, 2H), 8.14 (d, *J* = 8.1 Hz, 2H), 7.88 (d, *J* = 8.6 Hz, 2H), 7.82 (br, 2H), 7.64 (t, *J* = 5.9 Hz, 1H), 7.47 (d, *J* = 8.2 Hz, 2H), 4.48 (s, 2H), 2.81 (s, 3H), 2.76 (dd, *J* = 12.8, 6.6 Hz, 2H), 2.14 (t, *J* = 7.1 Hz, 2H), 1.56 – 1.26 (m, 13H).

6-((4-(5-Amino-6-(5-(4-(((tert-butoxycarbonyl)(methyl)amino)methyl)phenyl)-1,3,4-oxadiazol-2-yl)pyrazin-2-yl)phenyl)sulfonamido)hexanoic acid (12d). ^{1}H NMR (400 MHz, DMSO-d_6) δ 11.93 (s, 1H), 8.99 (s, 1H), 8.30 (d, *J* = 8.6 Hz, 2H), 8.14 (d, *J* = 8.1 Hz, 2H), 7.88 (d, *J* = 8.6 Hz, 2H), 7.83 (br, 2H), 7.62 (t, *J* = 5.1 Hz, 1H), 7.47 (d, *J* = 8.2 Hz, 2H), 4.48 (s, 2H), 2.81 (s, 3H), 2.75 (dd, *J* = 13.0, 6.8 Hz, 2H), 2.12 (t, *J* = 7.3 Hz, 2H), 1.49 – 1.31 (m, 13H), 1.27 – 1.16 (m, 2H).

7-((4-(5-Amino-6-(5-(4-(((tert-butoxycarbonyl)(methyl)amino)methyl)phenyl)-1,3,4-oxadiazol-2-yl)pyrazin-2-yl)phenyl)sulfonamido)heptanoic acid (12e). ^{1}H NMR (400 MHz, DMSO-d_6) δ 11.90 (s, 1H), 8.99 (s, 1H), 8.30 (d, *J* = 8.5 Hz, 2H), 8.15 (d, *J* = 8.1 Hz, 2H), 7.88 (d, *J* = 8.6 Hz, 2H), 7.83 (br, 2H), 7.61 (t, *J* = 5.8 Hz, 1H), 7.48 (d, *J* = 8.2 Hz, 2H), 4.48 (s, 2H), 2.81 (s, 3H), 2.75 (dd, *J* = 13.0, 6.8 Hz, 2H), 2.13 (t, *J* = 7.4 Hz, 2H), 1.52 – 1.30 (m, 13H), 1.27 – 1.12 (m, 4H).

5-((4-(5-Amino-6-(phenylcarbamoyl)pyrazin-2-yl)phenyl)sulfonamido)pentanoic acid (13a). ^{1}H NMR (400 MHz, DMSO-d_6) δ 11.96 (s, 1H), 10.41 (s, 1H), 8.98 (s, 1H), 8.42 (d, *J* = 8.5 Hz, 2H), 7.93 – 7.72 (m, 6H), 7.63 (t, *J* = 5.8 Hz, 1H), 7.39 (t, *J* = 7.9 Hz, 2H), 7.15 (t, *J* = 7.4 Hz, 1H), 2.74 (dd, *J* = 12.8, 6.5 Hz, 2H), 2.14 (t, *J* = 7.1 Hz, 2H), 1.52 – 1.31 (m, 4H).

6-((4-(5-Amino-6-(phenylcarbamoyl)pyrazin-2-yl)phenyl)sulfonamido)hexanoic acid (13b). ^{1}H NMR (400 MHz, DMSO-d_6) δ 11.93 (s, 1H), 10.40 (s, 1H), 8.98 (s, 1H), 8.42 (d, *J* = 8.4 Hz, 2H), 7.91 – 7.71 (m, 6H), 7.61 (t, *J* = 5.8 Hz, 1H), 7.38 (t, *J* = 7.8 Hz, 2H), 7.15 (t, *J* = 7.4 Hz, 1H), 2.73 (dd, *J* = 13.0, 6.6 Hz, 2H), 2.12 (t, *J* = 7.3 Hz, 2H), 1.46 – 1.31 (m, 4H), 1.27 – 1.15 (m, 2H).

7-((4-(5-Amino-6-(phenylcarbamoyl)pyrazin-2-yl)phenyl)sulfonamido)heptanoic acid (13c). ^{1}H NMR (400 MHz, DMSO-d_6) δ 11.95 (s, 1H), 10.40 (s, 1H), 8.98 (s, 1H), 8.42 (d, *J* = 8.5 Hz, 2H), 7.92 – 7.71 (m, 6H), 7.61 (t, *J* = 5.8 Hz, 1H), 7.38 (t, *J* = 7.9 Hz, 2H), 7.14 (t, *J* = 7.4 Hz, 1H), 2.73 (dd, *J* = 13.0, 6.8 Hz, 2H), 2.13 (t, *J* = 7.4 Hz, 2H), 1.47 – 1.30 (m, 4H), 1.25 – 1.12 (m, 4H).

8-((4-(5-Amino-6-(phenylcarbamoyl)pyrazin-2-yl)phenyl)sulfonamido)octanoic acid (13d). ^{1}H NMR (400 MHz, DMSO-d_6) δ 11.92 (s, 1H), 10.40 (s, 1H), 8.98 (s, 1H), 8.42 (d, *J* = 8.5 Hz, 2H), 7.95 – 7.73 (m, 6H), 7.60 (t, *J* = 5.8 Hz, 1H), 7.39 (t, *J* = 7.9 Hz, 2H), 7.15 (t, *J* = 7.4 Hz, 1H), 2.73 (dd, *J* = 13.0, 6.7 Hz, 2H), 2.13 (t, *J* = 7.4 Hz, 2H), 1.46 – 1.30 (m, 4H), 1.24 – 1.11 (m, 6H).

4.3.6 Synthesis and characterization of intermediates 13e and 13f

Pyrazine boronic ester derivative **11b** was coupled with the appropriate 4-bromobenzene sulfonamide derivatives **3e** and **3f** according to method VI, followed by ester hydrolysis according to method III to obtain the corresponding acids **13e** and **13f**.

3-(2-(2-((4-(5-Amino-6-(phenylcarbamoyl)pyrazin-2-yl)phenyl)sulfonamido)ethoxy) ethoxy)propanoic acid (13e). ^{1}H NMR (400 MHz, DMSO-d_6) δ 12.11 (br, 1H), 10.40 (s, 1H), 8.98 (s, 1H), 8.41 (d, *J* = 8.3 Hz, 2H), 7.95 – 7.68 (m, 7H), 7.38 (t, *J* = 7.7 Hz, 2H), 7.15 (t, *J* = 7.2 Hz, 1H), 3.55 (t, *J* = 6.2 Hz, 2H), 3.48 – 3.37 (m, 6H), 2.91 (dd, *J* = 11.3, 5.5 Hz, 2H), 2.39 (t, *J* = 6.2 Hz, 2H).

3-(2-(2-(2-((4-(5-Amino-6-(phenylcarbamoyl)pyrazin-2-yl)phenyl)sulfonamido)ethoxy) ethoxy)ethoxy)propanoic acid (13f). ^{1}H NMR (400 MHz, DMSO-d_6) δ 12.10 (br, 1H), 10.39 (s, 1H), 8.97 (s, 1H), 8.40 (d, *J* = 8.0 Hz, 2H), 7.91 – 7.69 (m, 7H), 7.37 (t, *J* = 7.5 Hz, 2H), 7.13 (t, *J* = 7.1 Hz, 1H), 3.54 (t, *J* = 6.0 Hz, 2H), 3.48 – 3.34 (m, 10H), 2.90 (dd, *J* = 11.3, 5.8 Hz, 2H), 2.38 (t, *J* = 6.0 Hz, 2H).

4.3.7 Synthesis and characterization of intermediates 29-31

Intermediate **28** was reacted with *N*-Boc-2-bromoethylamine to produce the corresponding alkylated derivative **29** according to method VIII, followed by a hydrogenation reaction according to method IX to produce the intermediate compound **30**. Finally, Boc-deprotection according to method VII-A afforded the phenyl-glutarimide derivative **31.**

Tert-butyl (2-(4-(2,6-bis(benzyloxy)pyridin-3-yl)phenoxy)ethyl)carbamate (29). ^{1}H NMR (400 MHz, DMSO-d_6) δ 7.69 (d, *J* = 8.1 Hz, 1H), 7.52 – 7.25 (m, 12H), 7.03 – 6.91 (m, 3H), 6.53 (d, *J* = 8.1 Hz, 1H), 5.40 (s, 2H), 5.36 (s, 2H), 3.98 (t, *J* = 5.8 Hz, 2H), 3.31 – 3.26 (m, 2H), 1.39 (s, 9H).

Tert-butyl (2-(4-(2,6-dioxopiperidin-3-yl)phenoxy)ethyl)carbamate (30). ^{1}H NMR (400 MHz, DMSO-d_6) δ 10.78 (s, 1H), 7.13 (d, *J* = 8.6 Hz, 2H), 7.01 – 6.95 (m, 1H), 6.89 (d, *J* = 8.6 Hz, 2H), 3.95 (t, *J* = 5.8 Hz, 2H), 3.79 (dd, *J* = 11.3, 4.9 Hz, 1H), 3.29 (dd, *J* = 11.8, 6.0 Hz, 2H), 2.69 – 2.59 (m, 1H), 2.50 – 2.41 (m, 1H), 2.21 – 2.10 (m, 1H), 2.06 – 1.96 (m, 1H), 1.39 (s, 9H).

3-(4-(2-Aminoethoxy)phenyl)piperidine-2,6-dione (31). ^{1}H NMR (400 MHz, DMSO-d_6) δ 10.77 (s, 1H), 8.37 – 8.13 (m, 3H), 7.14 (d, *J* = 8.7 Hz, 2H), 6.93 (d, *J* = 8.7 Hz, 2H), 4.16 (t, *J* = 5.2 Hz, 2H), 3.79 (dd, *J* = 11.4, 4.9 Hz, 1H), 3.24 – 3.09 (m, 2H), 2.68 – 2.58 (m, 1H), 2.48 – 2.41 (m, 1H), 2.21 – 2.07 (m, 1H), 2.04 – 1.94 (m, 1H).

4.3.8 Synthesis and characterization of intermediates 33-35.

The 6-fluoropicolinic acid **32** was refluxed in 5mL of thionyl chloride for 2 hours. Then the solvent was evaporated under reduced pressure to produce the corresponding acid chloride which was reacted with 3-aminopiperidine-2,6-dione according to method I to afford the intermediate compound **33**. The later was then converted to its piperazine analogue **34** through its reaction with 1-Boc-piperazine according to method XI. Finally, Boc-deprotection according to method VII-A afforded the picolinamide glutarimide derivative **35.**

N*-(2,6-dioxopiperidin-3-yl)-6-fluoropicolinamide *(33). ^{1}H NMR (400 MHz, DMSO-d_6) δ 10.84 (s, 1H), 8.97 (d, *J* = 8.5 Hz, 1H), 8.19 (dd, *J* = 15.6, 8.1 Hz, 1H), 8.03 – 7.95 (m, 1H), 7.44 (dd, *J* = 8.2, 1.8 Hz, 1H), 4.82 – 4.71 (m, 1H), 2.84 – 2.73 (m, 1H), 2.57 – 2.49 (m, 1H), 2.31 – 2.13 (m, 1H), 2.01 – 1.90 (m, 1H).

Tert-butyl 4-(6-((2,6-dioxopiperidin-3-yl)carbamoyl)pyridin-2-yl)piperazine-1-carboxylate (34). ^{1}H NMR (400 MHz, DMSO-d_6) δ 10.86 (s, 1H), 8.76 (d, *J* = 8.5 Hz, 1H), 7.70 (dd, *J* = 8.5, 7.3 Hz, 1H), 7.32 (d, *J* = 7.1 Hz, 1H), 7.03 (d, *J* = 8.5 Hz, 1H), 4.79 – 4.67 (m, 1H), 3.64 – 3.51 (m, 4H), 3.49 – 3.37 (m, 4H), 2.86 – 2.72 (m, 1H), 2.57 – 2.50 (m, 1H), 2.30 – 2.16 (m, 1H), 2.01 – 1.92 (m, 1H), 1.41 (s, 9H).

N-(2,6-dioxopiperidin-3-yl)-6-(piperazin-1-yl)picolinamide (35). ^{1}H NMR (400 MHz, DMSO-d_6) δ 10.86 (s, 1H), 9.48 (s, 2H), 8.80 (d, *J* = 8.5 Hz, 1H), 7.75 (dd, *J* = 8.5, 7.4 Hz,

1H), 7.38 (d, *J* = 7.2 Hz, 1H), 7.12 (d, *J* = 8.5 Hz, 1H), 4.81 – 4.65 (m, 1H), 3.92 – 3.78 (m, 4H), 3.16 (s, 4H), 2.86 – 2.71 (m, 1H), 2.59 – 2.49 (m, 1H), 2.32 – 2.14 (m, 1H), 2.02 – 1.91 (m, 1H).

4.3.9 Synthesis and characterization of the final PROTACs

The linker-connected ATR inhibitors (**12a-e** and **13a-f)** were reacted with the appropriate E3 ligase ligand (**20a-c, 25, 31, 35** and **41),** according to method IV. In case of coupling with **12c-d, t**he amide coupling reaction was followed by the removal of Boc-protecting group according to method VII-B.

6-((4-(5-Amino-6-(5-phenyl-1,3,4-oxadiazol-2-yl)pyrazin-2-yl)phenyl)sulfonamido)-N-(3-(2-(2,6-dioxopiperidin-3-yl)-1-oxoisoindolin-4-yl)prop-2-yn-1-yl)hexanamide 42a (Abd117).

^{1}H NMR (400 MHz, DMSO-d_6) δ 10.97 (s, 1H), 8.99 (s, 1H), 8.29 (d, *J* = 8.5 Hz, 3H), 8.16 (dd, *J* = 7.6, 1.8 Hz, 2H), 7.88 (d, *J* = 8.5 Hz, 2H), 7.84 (br, 2H), 7.74 – 7.56 (m, 6H), 7.50 (t, *J* = 7.6 Hz, 1H), 5.12 (dd, *J* = 13.3, 5.1 Hz, 1H), 4.41 (d, *J* = 17.7 Hz, 1H), 4.28 (d, *J* = 17.7 Hz, 1H), 4.12 (d, *J* = 5.3 Hz, 2H), 2.96 – 2.82 (m, 1H), 2.74 (dd, *J* = 13.0, 6.7 Hz, 2H), 2.63 – 2.50 (m, 1H), 2.45 – 2.31 (m, 1H), 2.06 (t, *J* = 7.4 Hz, 2H), 2.03 – 1.93 (m, 1H), 1.47 – 1.31 (m, 4H), 1.29 – 1.19 (m, 2H). ^{13}C NMR (101 MHz, DMSO-d_6) δ 173.24, 172.30, 171.38, 167.95, 164.43, 163.29, 153.25, 144.37, 144.22, 140.30, 139.89, 138.60, 134.57, 132.87, 132.44, 130.00, 129.10, 127.57, 127.41, 126.22, 123.62, 123.48, 120.21, 118.31, 93.02, 77.77, 52.05, 47.32, 42.91, 35.42, 31.62, 29.26, 29.06, 26.19, 25.11, 22.88. HRMS (ESI, positive): Calcd. for $C_{40}H_{38}N_9O_7S$ $[M+H]^+$: *m/z* = 788.261; Found: 788.262. HPLC t_R = 13.49 min (purity 95.0%).

5-((4-(5-Amino-6-(5-phenyl-1,3,4-oxadiazol-2-yl)pyrazin-2-yl)phenyl)sulfonamido)-N-(3-(2-(2,6-dioxopiperidin-3-yl)-1-oxoisoindolin-4-yl)prop-2-yn-1-yl)pentanamide 42b (Abd120).

^{1}H NMR (400 MHz, DMSO-d_6) δ 10.99 (s, 1H), 8.99 (s, 1H), 8.31 (dd, *J* = 12.5, 6.9 Hz, 3H), 8.15 (dd, *J* = 7.7, 1.7 Hz, 2H), 7.88 (d, *J* = 8.5 Hz, 2H), 7.84 (br, 2H), 7.73 – 7.58 (m, 6H), 7.50 (t, *J* = 7.6 Hz, 1H), 5.12 (dd, *J* = 13.3, 5.1 Hz, 1H), 4.41 (d, *J* = 17.8 Hz, 1H), 4.28 (d, *J* = 17.8 Hz, 1H), 4.12 (d, *J* = 5.3 Hz, 2H), 2.95 – 2.84 (m, 1H), 2.76 (dd, *J* = 13.0, 6.7 Hz, 2H), 2.62 – 2.51 (m, 1H), 2.46 – 2.34 (m, 1H), 2.07 (t, *J* = 7.2 Hz, 2H), 2.02 – 1.95 (m, 1H), 1.53 – 1.43 (m, 2H), 1.43 – 1.32 (m, 2H). ^{13}C NMR (101 MHz, DMSO-d_6) δ 173.28, 172.17,

171.41, 167.96, 164.41, 163.26, 153.23, 144.35, 144.21, 140.30, 139.88, 138.57, 134.60, 132.87, 132.43, 129.99, 129.10, 127.57, 127.39, 126.21, 123.63, 123.46, 120.18, 118.28, 92.93, 77.80, 52.05, 47.33, 42.79, 34.95, 31.61, 29.12, 29.07, 22.87, 22.74. HRMS (ESI, positive): Calcd. for $C_{39}H_{36}N_9O_7S$ $[M+H]^+$: *m/z* = 774.245; Found: 774.245. HPLC t_R = 13.31 min (purity 100%).

1-(4-(5-(3-Amino-6-(4-(N-(5-((5-(2-(2,6-dioxopiperidin-3-yl)-1-oxoisoindolin-4-yl)pent-4-yn-1-yl)amino)-5-oxopentyl)sulfamoyl)phenyl)pyrazin-2-yl)-1,3,4-oxadiazol-2-yl)phenyl)-N-methylmethanaminium formate 42c (Abd123).

^{1}H NMR (400 MHz, DMSO-d_6) δ 10.93 (br, 1H), 8.99 (s, 1H), 8.30 (d, *J* = 8.6 Hz, 2H), 8.24 (s, 1H), 8.12 (d, *J* = 8.3 Hz, 2H), 7.93 – 7.74 (m, 5H), 7.64 (dd, *J* = 11.1, 4.6 Hz, 4H), 7.56 (dd, *J* = 7.6, 1.0 Hz, 1H), 7.46 (t, *J* = 7.6 Hz, 1H), 5.11 (dd, *J* = 13.2, 5.1 Hz, 1H), 4.42 (d, *J* = 17.9 Hz, 1H), 4.28 (d, *J* = 17.9 Hz, 1H), 3.89 (s, 2H), 3.14 (dd, *J* = 13.0, 6.6 Hz, 2H), 2.94 – 2.83 (m, 1H), 2.75 (t, *J* = 6.5 Hz, 2H), 2.59 – 2.52 (m, 1H), 2.43 (dd, *J* = 12.7, 5.7 Hz, 3H), 2.37 (s, 3H), 2.02 – 1.93 (m, 3H), 1.67 – 1.57 (m, 2H), 1.49 – 1.39 (m, 2H), 1.39 – 1.29 (m, 2H). ^{13}C NMR (101 MHz, DMSO-d_6) δ 173.26, 172.21, 171.37, 168.07, 164.57, 164.35, 163.20, 153.24, 144.32, 144.18, 143.32, 140.38, 139.87, 138.57, 134.28, 132.35, 129.93, 128.93, 127.56, 127.38, 126.20, 123.02, 122.34, 120.19, 119.12, 96.15, 77.01, 53.82, 52.03, 47.41, 42.81, 37.95, 35.23, 34.89, 31.65, 29.17, 28.63, 22.82, 22.74, 16.86. HRMS (ESI, positive): Calcd. for $C_{43}H_{45}N_{10}O_7S$ $[M+H]^+$: *m/z* = 845.319; Found: 845.319. HPLC t_R = 11.16 min (purity 95.3%).

1-(4-(5-(3-Amino-6-(4-(N-(6-((5-(2-(2,6-dioxopiperidin-3-yl)-1-oxoisoindolin-4-yl)pent-4-yn-1-yl)amino)-6-oxohexyl)sulfamoyl)phenyl)pyrazin-2-yl)-1,3,4-oxadiazol-2-yl)phenyl)-N-methylmethanaminium formate 42d (Abd132).

^{1}H NMR (400 MHz, DMSO-d_6) δ 10.93 (br, 1H), 8.99 (s, 1H), 8.29 (d, *J* = 8.6 Hz, 2H), 8.22 (s, 1H), 8.16 (d, *J* = 8.3 Hz, 2H), 7.93 – 7.74 (m, 5H), 7.70 – 7.55 (m, 5H), 7.47 (t, *J* = 7.6 Hz, 1H), 5.11 (dd, *J* = 13.1, 5.1 Hz, 1H), 4.43 (d, *J* = 17.9 Hz, 1H), 4.28 (d, *J* = 17.9 Hz, 1H), 4.05 (s, 2H), 3.15 (dd, *J* = 12.8, 6.6 Hz, 2H), 2.94 – 2.84 (m, 1H), 2.74 (t, *J* = 6.3 Hz, 2H), 2.60 – 2.51 (m, 1H), 2.47 – 2.37 (m, 6H), 1.99 (t, *J* = 7.3 Hz, 3H), 1.68 – 1.59 (m, 2H), 1.44 – 1.32 (m, 4H), 1.24 – 1.14 (m, 2H). ^{13}C NMR (101 MHz, DMSO-d_6) δ 173.25, 172.40, 171.38, 168.08, 164.49, 164.21, 163.30, 153.26, 144.32, 144.25, 140.48, 140.32, 139.87, 138.60, 134.31, 132.36, 130.51, 128.95, 127.57, 127.52, 126.22, 123.01, 120.14, 119.15, 96.18, 77.00, 52.72, 52.04, 47.42, 42.94, 37.93, 35.70, 33.95, 31.66, 29.23, 28.59, 26.21,

25.22, 22.75, 16.85. HRMS (ESI, positive): Calcd. for $C_{44}H_{47}N_{10}O_7S$ $[M+H]^+$: *m/z* = 859.334; Found: 859.334. HPLC t_R = 12.12 min (purity 95.4%).

1-(4-(5-(3-Amino-6-(4-(N-(7-((5-(2-(2,6-dioxopiperidin-3-yl)-1-oxoisoindolin-4-yl)pent-4-yn-1-yl)amino)-7-oxoheptyl)sulfamoyl)phenyl)pyrazin-2-yl)-1,3,4-oxadiazol-2-yl)phenyl)-N-methylmethanaminium formate 42e (Abd133).

^{1}H NMR (400 MHz, DMSO-d_6) δ 10.94 (br, 1H), 8.99 (s, 1H), 8.31 – 8.25 (m, 3H), 8.12 (d, *J* = 8.2 Hz, 2H), 7.96 – 7.72 (m, 5H), 7.70 – 7.54 (m, 5H), 7.47 (t, *J* = 7.6 Hz, 1H), 5.11 (dd, *J* = 13.1, 5.1 Hz, 1H), 4.43 (d, *J* = 17.9 Hz, 1H), 4.28 (d, *J* = 17.8 Hz, 1H), 3.89 (s, 2H), 3.15 (dd, *J* = 12.8, 6.7 Hz, 2H), 2.95 – 2.84 (m, 1H), 2.74 (t, *J* = 6.6 Hz, 2H), 2.60 – 2.52 (m, 1H), 2.43 (t, *J* = 7.0 Hz, 3H), 2.37 (s, 3H), 1.99 (t, *J* = 7.4 Hz, 3H), 1.69 – 1.58 (m, 2H), 1.45 – 1.30 (m, 4H), 1.24 – 1.08 (m, 4H). ^{13}C NMR (101 MHz, DMSO-d_6) δ 173.24, 172.47, 171.38, 168.09, 164.81, 164.36, 163.21, 153.24, 144.32, 144.18, 143.41, 140.35, 139.88, 138.59, 134.32, 132.37, 129.91, 128.95, 127.57, 127.38, 126.21, 123.04, 122.32, 120.20, 119.16, 96.17, 77.00, 53.84, 52.03, 47.42, 42.98, 37.92, 35.73, 34.91, 31.66, 29.35, 28.60, 26.22, 25.54, 22.75, 16.85. HRMS (ESI, positive): Calcd. for $C_{45}H_{49}N_{10}O_7S$ $[M+H]^+$: *m/z* = 873.350; Found: 873.350. HPLC t_R = 12.41 min (purity 95.9%).

1-(4-(5-(3-Amino-6-(4-(N-(7-((3-(2-(2,6-dioxopiperidin-3-yl)-1-oxoisoindolin-4-yl)prop-2-yn-1-yl)amino)-7-oxoheptyl)sulfamoyl)phenyl)pyrazin-2-yl)-1,3,4-oxadiazol-2-yl)phenyl)-N-methylmethanaminium formate 42f (Abd134).

^{1}H NMR (400 MHz, DMSO-d_6) δ 10.91 (br, 1H), 8.92 (s, 1H), 8.22 (d, *J* = 8.5 Hz, 3H), 8.17 (s, 1H), 8.06 (d, *J* = 8.2 Hz, 2H), 7.81 (d, *J* = 8.4 Hz, 2H), 7.76 (br, 2H), 7.64 (d, *J* = 7.6 Hz, 1H), 7.60 – 7.49 (m, 4H), 7.43 (t, *J* = 7.6 Hz, 1H), 5.05 (dd, *J* = 13.3, 5.0 Hz, 1H), 4.34 (d, *J* = 17.7 Hz, 1H), 4.20 (d, *J* = 17.8 Hz, 1H), 4.04 (d, *J* = 5.3 Hz, 2H), 3.82 (s, 2H), 2.88 – 2.76 (m, 1H), 2.72 – 2.63 (m, 2H), 2.56 – 2.45 (m, 1H), 2.38 – 2.22 (m, 4H), 1.99 (t, *J* = 7.4 Hz, 2H), 1.96 – 1.88 (m, 1H), 1.41 – 1.32 (m, 2H), 1.32 – 1.23 (m, 2H), 1.19 – 1.04 (m, 4H). ^{13}C NMR (101 MHz, DMSO-d_6) δ 173.15, 172.29, 171.29, 167.86, 164.47, 164.28, 163.12, 153.15, 144.26, 144.10, 143.40, 140.27, 139.79, 138.50, 134.46, 132.34, 129.80, 129.01, 127.48, 127.30, 126.13, 123.52, 122.22, 120.12, 118.22, 92.95, 77.65, 53.81, 51.95, 47.21, 42.87, 35.34, 34.88, 31.52, 29.21, 28.95, 28.47, 26.12, 25.33, 22.80. HRMS (ESI, positive): Calcd. for $C_{43}H_{45}N_{10}O_7S$ $[M+H]^+$: *m/z* = 845.319; Found: 845.318. HPLC t_R = 11.99 min (purity 94.2%).

1-(4-(5-(3-Amino-6-(4-(N-(6-((3-(2-(2,6-dioxopiperidin-3-yl)-1-oxoisoindolin-4-yl)prop-2-yn-1-yl)amino)-6-oxohexyl)sulfamoyl)phenyl)pyrazin-2-yl)-1,3,4-oxadiazol-2-yl)phenyl)-N-methylmethanaminium formate 42g (Abd136).

^{1}H NMR (400 MHz, DMSO-d_6) δ 10.94 (br, 1H), 8.99 (s, 1H), 8.30 (m, 3H), 8.22 (s, 1H), 8.14 (d, *J* = 8.2 Hz, 2H), 7.88 (d, *J* = 8.5 Hz, 2H), 7.84 (br, 2H), 7.71 (d, *J* = 7.5 Hz, 1H), 7.63 (dd, *J* = 13.0, 7.9 Hz, 4H), 7.50 (t, *J* = 7.6 Hz, 1H), 5.12 (dd, *J* = 13.3, 5.1 Hz, 1H), 4.41 (d, *J* = 17.7 Hz, 1H), 4.28 (d, *J* = 17.7 Hz, 1H), 4.12 (d, *J* = 5.3 Hz, 2H), 3.93 (s, 2H), 2.96 – 2.83 (m, 1H), 2.74 (t, *J* = 6.0 Hz, 2H), 2.62 – 2.51 (m, 1H), 2.45 – 2.29 (m, 4H), 2.06 (t, *J* = 7.4 Hz, 2H), 2.02 – 1.94 (m, 1H), 1.48 – 1.32 (m, 4H), 1.27 – 1.16 (m, 2H). ^{13}C NMR (101 MHz, DMSO-d_6) δ 173.24, 172.30, 171.39, 167.95, 164.47, 164.34, 163.24, 153.26, 144.37, 144.22, 140.30, 139.89, 138.60, 134.57, 132.44, 130.05, 129.10, 127.58, 127.43, 126.23, 123.62, 122.49, 120.20, 118.31, 93.03, 77.77, 53.63, 52.05, 47.32, 42.91, 35.42, 34.74, 31.62, 29.25, 29.06, 26.19, 25.12, 22.88. HRMS (ESI, positive): Calcd. for $C_{42}H_{43}N_{10}O_7S$ $[M+H]^+$: *m/z* = 831.303; Found: 831.303. HPLC t_R = 11.68 min (purity 95.1%).

3-Amino-6-(4-(N-(6-((3-(2-(2,6-dioxopiperidin-3-yl)-1-oxoisoindolin-4-yl)prop-2-yn-1-yl)amino)-6-oxohexyl)sulfamoyl)phenyl)-N-phenylpyrazine-2-carboxamide 42h (Abd108).

^{1}H NMR (400 MHz, DMSO-d_6) δ 10.98 (s, 1H), 10.40 (s, 1H), 8.98 (s, 1H), 8.41 (d, *J* = 8.5 Hz, 2H), 8.30 (t, *J* = 5.3 Hz, 1H), 7.91 – 7.75 (m, 6H), 7.72 (d, *J* = 7.1 Hz, 1H), 7.65 – 7.57 (m, 2H), 7.51 (t, *J* = 7.6 Hz, 1H), 7.38 (t, *J* = 7.9 Hz, 2H), 7.15 (t, *J* = 7.4 Hz, 1H), 5.13 (dd, *J* = 13.3, 5.1 Hz, 1H), 4.42 (d, *J* = 17.8 Hz, 1H), 4.29 (d, *J* = 17.7 Hz, 1H), 4.12 (d, *J* = 5.3 Hz, 2H), 2.95 – 2.83 (m, 1H), 2.72 (dd, *J* = 13.0, 6.7 Hz, 2H), 2.64 – 2.52 (m, 1H), 2.46 – 2.33 (m, 1H), 2.06 (t, *J* = 7.4 Hz, 2H), 2.02 – 1.94 (m, 1H), 1.48 – 1.32 (m, 4H), 1.28 – 1.17 (m, 2H). ^{13}C NMR (101 MHz, DMSO-d_6) δ 173.24, 172.29, 171.39, 167.96, 164.82, 155.09, 145.65, 144.38, 140.08, 139.78, 138.27, 137.17, 134.59, 132.46, 129.11, 129.05, 127.31, 126.57, 124.77, 124.72, 123.63, 121.68, 118.32, 93.03, 77.79, 52.06, 47.33, 42.91, 35.42, 31.62, 29.25, 29.06, 26.20, 25.11, 22.89. HRMS (ESI, positive): Calcd. for $C_{39}H_{39}N_8O_7S$ $[M+H]^+$: *m/z* = 763.266; Found: 763.266. HPLC t_R = 13.11 min (purity 96.6%).

3-Amino-6-(4-(N-(6-((5-(2-(2,6-dioxopiperidin-3-yl)-1-oxoisoindolin-4-yl)pent-4-yn-1-yl)amino)-6-oxohexyl)sulfamoyl)phenyl)-N-phenylpyrazine-2-carboxamide 42i (Abd110).

^{1}H NMR (400 MHz, DMSO-d_6) δ 10.95 (s, 1H), 10.40 (s, 1H), 8.97 (s, 1H), 8.41 (d, *J* = 8.5 Hz, 2H), 7.88 – 7.74 (m, 7H), 7.68 (d, *J* = 7.4 Hz, 1H), 7.63 – 7.56 (m, 2H), 7.48 (t, *J* = 7.6 Hz, 1H), 7.38 (t, *J* = 7.9 Hz, 2H), 7.14 (t, *J* = 7.4 Hz, 1H), 5.12 (dd, *J* = 13.1, 5.0 Hz, 1H), 4.44 (d, *J* = 17.9 Hz, 1H), 4.29 (d, *J* = 17.9 Hz, 1H), 3.16 (dd, *J* = 12.7, 6.6 Hz, 2H), 2.95 – 2.84 (m, 1H), 2.72 (dd, *J* = 13.0, 6.7 Hz, 2H), 2.61 – 2.50 (m, 1H), 2.45 (t, *J* = 7.2 Hz, 3H), 1.99 (t, *J* = 7.3 Hz, 3H), 1.72 – 1.60 (m, 2H), 1.44 – 1.29 (m, 4H), 1.24 – 1.14 (m, 2H). ^{13}C NMR (101 MHz, DMSO-d_6) δ 173.26, 172.40, 171.39, 168.10, 164.81, 155.08, 145.63, 144.33, 140.10, 139.78, 138.26, 137.17, 134.35, 132.38, 129.05, 128.97, 127.32, 126.56, 124.76, 123.05, 121.66, 119.18, 96.20, 77.02, 52.04, 47.43, 42.94, 37.95, 35.71, 31.65, 29.24, 28.61, 26.23, 25.23, 22.76, 16.86. HRMS (ESI, positive): Calcd. for $C_{41}H_{43}N_8O_7S$ $[M+H]^+$: *m/z* = 791.297; Found: 791.296. HPLC t_R = 13.51 min (purity 97.4%).

3-Amino-6-(4-(N-(7-((5-(2-(2,6-dioxopiperidin-3-yl)-1-oxoisoindolin-4-yl)pent-4-yn-1-yl)amino)-7-oxoheptyl)sulfamoyl)phenyl)-N-phenylpyrazine-2-carboxamide 42j (Abd127).

^{1}H NMR (400 MHz, DMSO-d_6) δ 10.95 (s, 1H), 10.40 (s, 1H), 8.98 (s, 1H), 8.41 (d, *J* = 8.6 Hz, 2H), 7.89 – 7.72 (m, 7H), 7.68 (dd, *J* = 7.5, 0.7 Hz, 1H), 7.60 (t, *J* = 6.1 Hz, 2H), 7.48 (t, *J* = 7.6 Hz, 1H), 7.41 – 7.34 (m, 2H), 7.14 (t, *J* = 7.4 Hz, 1H), 5.12 (dd, *J* = 13.1, 5.1 Hz, 1H), 4.44 (d, *J* = 17.9 Hz, 1H), 4.29 (d, *J* = 17.8 Hz, 1H), 3.16 (dd, *J* = 12.8, 6.7 Hz, 2H), 2.96 – 2.84 (m, 1H), 2.73 (dd, *J* = 13.1, 6.7 Hz, 2H), 2.61 – 2.51 (m, 1H), 2.44 (t, *J* = 6.9 Hz, 3H), 2.03 – 1.93 (m, 3H), 1.71 – 1.59 (m, 2H), 1.43 – 1.30 (m, 4H), 1.24 – 1.10 (m, 4H). ^{13}C NMR (101 MHz, DMSO-d_6) δ 173.25, 172.48, 171.39, 168.10, 164.80, 155.08, 145.62, 144.33, 140.14, 139.77, 138.26, 137.17, 134.34, 132.38, 129.04, 128.96, 127.31, 126.55, 124.76, 124.71, 123.05, 121.66, 119.18, 96.19, 77.02, 52.04, 47.43, 42.98, 37.93, 35.74, 31.66, 29.34, 28.61, 26.24, 25.55, 22.76, 16.86. HRMS (ESI, positive): Calcd. for $C_{42}H_{45}N_8O_7S$ $[M+H]^+$: *m/z* = 805.313; Found: 805.314. HPLC t_R = 13.83 min (purity 97.2%).

3-Amino-6-(4-(N-(5-((5-(2-(2,6-dioxopiperidin-3-yl)-1-oxoisoindolin-4-yl)pent-4-yn-1-yl)amino)-5-oxopentyl)sulfamoyl)phenyl)-N-phenylpyrazine-2-carboxamide 42k (Abd130).

^{1}H NMR (500 MHz, DMSO-d_6) δ 11.00 (s, 1H), 10.44 (s, 1H), 9.03 (s, 1H), 8.46 (d, *J* = 8.5 Hz, 2H), 7.92 – 7.79 (m, 7H), 7.72 (d, *J* = 7.6 Hz, 1H), 7.70 – 7.61 (m, 2H), 7.53 (t, *J* = 7.6 Hz, 1H), 7.43 (t, *J* = 7.9 Hz, 2H), 7.22 – 7.17 (m, 1H), 5.17 (dd, *J* = 13.3, 4.9 Hz, 1H), 4.48 (d, *J* = 17.8 Hz, 1H), 4.34 (d, *J* = 17.8 Hz, 1H), 3.20 (dd, *J* = 12.6, 6.3 Hz, 2H), 2.99 – 2.89 (m, 1H), 2.78 (dd, *J* = 12.9, 6.5 Hz, 2H), 2.65 – 2.55 (m, 1H), 2.49 (t, *J* = 7.0 Hz, 3H), 2.04 (t, *J* = 7.0 Hz, 3H), 1.73 – 1.64 (m, 2H), 1.53 – 1.45 (m, 2H), 1.44 – 1.35 (m, 2H). ^{13}C NMR (126 MHz, DMSO-d_6) δ 173.34, 172.29, 171.46, 168.16, 164.87, 155.15, 145.70, 144.40, 140.20, 139.84, 138.33, 137.24, 134.40, 132.45, 129.12, 129.04, 127.37, 126.62, 124.78, 123.12, 121.74, 119.23, 96.26, 77.09, 52.11, 47.50, 42.87, 38.03, 35.32, 31.72, 29.25, 28.70, 22.91, 22.82, 16.94. HRMS (ESI, positive): Calcd. for $C_{40}H_{41}N_8O_7S$ $[M+H]^+$: *m/z* = 777.2813; Found: 777.2819. HPLC t_R = 13.72 min (purity 93.6%)

3-Amino-6-(4-(N-(8-((3-(2-(2,6-dioxopiperidin-3-yl)-1-oxoisoindolin-4-yl)prop-2-yn-1-yl)amino)-8-oxooctyl)sulfamoyl)phenyl)-N-phenylpyrazine-2-carboxamide 42l (Abd139).

^{1}H NMR (400 MHz, DMSO-d_6) δ 10.98 (s, 1H), 10.40 (s, 1H), 8.98 (s, 1H), 8.42 (d, *J* = 8.5 Hz, 2H), 8.29 (t, *J* = 5.2 Hz, 1H), 7.88 – 7.75 (m, 6H), 7.72 (d, *J* = 7.5 Hz, 1H), 7.61 (dd, *J* = 11.0, 6.6 Hz, 2H), 7.51 (t, *J* = 7.6 Hz, 1H), 7.38 (t, *J* = 7.9 Hz, 2H), 7.15 (t, *J* = 7.4 Hz, 1H), 5.13 (dd, *J* = 13.3, 5.1 Hz, 1H), 4.42 (d, *J* = 17.7 Hz, 1H), 4.29 (d, *J* = 17.8 Hz, 1H), 4.12 (d, *J* = 5.3 Hz, 2H), 2.95 – 2.84 (m, 1H), 2.72 (dd, *J* = 12.8, 6.6 Hz, 2H), 2.62 – 2.53 (m, 1H), 2.45 – 2.29 (m, 1H), 2.10 – 1.93 (m, 3H), 1.49 – 1.41 (m, 2H), 1.38 – 1.30 (m, 2H), 1.26 – 1.09 (m, 6H). ^{13}C NMR (101 MHz, DMSO-d_6) δ 173.23, 172.42, 171.39, 167.96, 164.82, 155.09, 145.63, 144.38, 140.16, 139.77, 138.26, 137.17, 134.57, 132.46, 129.11, 129.05, 127.31, 126.55, 124.76, 124.73, 123.63, 121.69, 118.34, 93.09, 77.75, 52.05, 47.31, 42.97, 35.51, 31.63, 29.41, 29.04, 28.93, 28.70, 26.37, 25.48, 22.89. HRMS (ESI, positive): Calcd. for $C_{41}H_{43}N_8O_7S$ $[M+H]^+$: *m/z* = 791.297; Found: 791.299. HPLC t_R = 14.14 min (purity 96.3%).

3-Amino-6-(4-(N-(6-((5-(2-(1-methyl-2,6-dioxopiperidin-3-yl)-1-oxoisoindolin-4-yl)pent-4-yn-1-yl)amino)-6-oxohexyl)sulfamoyl)phenyl)-N-phenylpyrazine-2-carboxamide 42m (Abd140).

^{1}H NMR (400 MHz, DMSO-d_6) δ 10.40 (s, 1H), 8.98 (s, 1H), 8.41 (d, *J* = 8.5 Hz, 2H), 7.89 – 7.73 (m, 7H), 7.69 (d, *J* = 7.5 Hz, 1H), 7.60 (t, *J* = 6.1 Hz, 2H), 7.49 (t, *J* = 7.6 Hz, 1H), 7.38 (t, *J* = 7.9 Hz, 2H), 7.14 (t, *J* = 7.4 Hz, 1H), 5.19 (dd, *J* = 13.4, 5.0 Hz, 1H), 4.43 (d, *J* = 17.8 Hz, 1H), 4.30 (d, *J* = 17.9 Hz, 1H), 3.16 (dd, *J* = 13.0, 6.5 Hz, 2H), 3.03 – 2.91 (m, 4H), 2.78 – 2.66 (m, 3H), 2.44 (t, *J* = 7.0 Hz, 3H), 1.98 (t, *J* = 7.4 Hz, 3H), 1.70 – 1.59 (m, 2H), 1.44 – 1.32 (m, 4H), 1.23 – 1.14 (m, 2H). ^{13}C NMR (101 MHz, DMSO-d_6) δ 172.37, 172.29, 171.00, 168.13, 164.81, 155.09, 145.63, 144.39, 140.10, 139.78, 138.26, 137.17, 134.36, 132.37, 129.04, 128.98, 127.31, 126.55, 124.76, 124.71, 123.10, 121.66, 119.18, 96.17, 77.07, 52.52, 47.41, 42.94, 37.95, 35.73, 31.80, 29.24, 28.60, 27.01, 26.24, 25.22, 22.04, 16.87. HRMS (ESI, positive): Calcd. for $C_{42}H_{45}N_8O_7S$ $[M+H]^+$: *m/z* = 805.313; Found: 805.312. HPLC t_R = 14.27 min (purity 98.9%).

4-(5-Amino-6-(5-phenyl-1,3,4-oxadiazol-2-yl)pyrazin-2-yl)-N-(6-(4-(2-(2,6-dioxopiperidin-3-yl)-1,3-dioxoisoindolin-5-yl)piperazin-1-yl)-6-oxohexyl)benzenesulfonamide 43a (Abd116).

^{1}H NMR (400 MHz, DMSO-d_6) δ 11.05 (s, 1H), 8.99 (s, 1H), 8.30 (d, *J* = 8.6 Hz, 2H), 8.14 (dt, *J* = 10.3, 4.9 Hz, 2H), 7.89 (d, *J* = 8.6 Hz, 2H), 7.82 (br, 2H), 7.72 – 7.57 (m, 5H), 7.26 (d, *J* = 2.1 Hz, 1H), 7.16 (dd, *J* = 8.6, 2.2 Hz, 1H), 5.05 (dd, *J* = 12.9, 5.4 Hz, 1H), 3.54 (s, 4H), 3.48 – 3.34 (m, 4H), 2.94 – 2.80 (m, 1H), 2.77 (dd, *J* = 12.9, 6.7 Hz, 2H), 2.63 – 2.51 (m, 2H), 2.26 (t, *J* = 7.4 Hz, 2H), 2.04 – 1.95 (m, 1H), 1.49 – 1.33 (m, 4H), 1.30 – 1.17 (m, 2H). ^{13}C NMR (101 MHz, DMSO-d_6) δ 173.21, 171.16, 170.48, 167.92, 167.37, 164.40, 163.25, 155.22, 153.24, 144.21, 140.41, 139.88, 138.58, 134.25, 132.86, 129.98, 127.59, 127.39, 126.20, 125.31, 123.46, 120.18, 118.89, 118.11, 108.27, 49.23, 47.20, 46.94, 44.47, 42.91, 32.49, 31.43, 29.26, 26.22, 24.60, 22.62. HRMS (ESI, positive): Calcd. for $C_{41}H_{41}N_{10}O_8S$ $[M+H]^+$: *m/z* = 833.282; Found: 833.283. HPLC t_R = 13.52 min (purity 99.7%).

4-(5-Amino-6-(5-phenyl-1,3,4-oxadiazol-2-yl)pyrazin-2-yl)-N-(5-(4-(2-(2,6-dioxopiperidin-3-yl)-1,3-dioxoisoindolin-5-yl)piperazin-1-yl)-5-oxopentyl)benzenesulfonamide 43b (Abd118).

^{1}H NMR (400 MHz, DMSO-d_6) δ 11.05 (s, 1H), 8.98 (s, 1H), 8.29 (d, *J* = 8.5 Hz, 2H), 8.18 – 8.09 (m, 2H), 7.89 (d, *J* = 8.5 Hz, 2H), 7.81 (br, 2H), 7.73 – 7.54 (m, 5H), 7.22 (d, *J* = 1.9 Hz, 1H), 7.12 (dd, *J* = 8.6, 2.1 Hz, 1H), 5.05 (dd, *J* = 12.9, 5.4 Hz, 1H), 3.53 (s, 4H), 3.45 – 3.32 (m, 4H), 2.94 – 2.75 (m, 3H), 2.63 – 2.50 (m, 2H), 2.25 (t, *J* = 7.0 Hz, 2H), 2.07 – 1.96 (m, 1H), 1.52 – 1.36 (m, 4H). ^{13}C NMR (101 MHz, DMSO-d_6) δ 173.21, 171.04, 170.48, 167.88, 167.35, 164.38, 163.22, 155.16, 153.22, 144.17, 140.40, 139.87, 138.54, 134.22, 132.84, 129.96, 127.59, 127.36, 126.17, 125.26, 123.44, 120.16, 118.88, 118.02, 108.19, 55.34, 49.22, 47.17, 46.91, 44.45, 42.79, 32.01, 31.43, 29.03, 22.63, 22.19. HRMS (ESI, positive): Calcd. for $C_{40}H_{39}N_{10}O_8S$ $[M+H]^+$: *m/z* = 819.267; Found: 819.269. HPLC t_R = 13.11 min (purity 99.7%).

4-(5-Amino-6-(5-(4-((methylamino)methyl)phenyl)-1,3,4-oxadiazol-2-yl)pyrazin-2-yl)-N-(5-(4-(2-(2,6-dioxopiperidin-3-yl)-1,3-dioxoisoindolin-5-yl)piperazin-1-yl)-5-oxopentyl)benzenesulfonamide 43c (Abd122).

^{1}H NMR (400 MHz, DMSO-d_6) δ 11.02 (br, 1H), 9.01 (s, 1H), 8.32 (d, *J* = 8.3 Hz, 2H), 8.10 (d, *J* = 8.0 Hz, 2H), 7.92 (d, *J* = 8.4 Hz, 2H), 7.83 (br, 2H), 7.71 – 7.53 (m, 4H), 7.25 (s, 1H), 7.16 (d, *J* = 8.6 Hz, 1H), 5.07 (dd, *J* = 12.9, 5.4 Hz, 1H), 3.80 (s, 2H), 3.55 (s, 4H), 3.48 – 3.35 (m, 4H), 2.95 – 2.77 (m, 3H), 2.64 – 2.52 (m, 2H), 2.32 (s, 3H), 2.28 (t, *J* = 7.1 Hz, 2H), 2.08 – 1.99 (m, 1H), 1.55 – 1.38 (m, 4H). ^{13}C NMR (101 MHz, DMSO-d_6) δ 173.23, 171.06, 170.50, 167.91, 167.38, 164.46, 163.12, 155.20, 153.24, 144.16, 140.43, 139.91, 138.56, 134.25, 129.46, 127.62, 127.29, 126.21, 125.29, 121.85, 120.24, 118.91, 118.06, 108.23, 54.85, 49.25, 47.21, 46.94, 46.17, 44.49, 42.82, 35.82, 32.04, 31.45, 29.05, 22.64, 22.21. HRMS (ESI, positive): Calcd. for $C_{42}H_{44}N_{11}O_8S$ $[M+H]^+$: *m/z* = 862.309; Found: 862.309. HPLC t_R = 10.62 min (purity 97.5%).

1-(4-(5-(3-Amino-6-(4-(N-(6-(4-(2-(2,6-dioxopiperidin-3-yl)-1,3-dioxoisoindolin-5-yl)piperazin-1-yl)-6-oxohexyl)sulfamoyl)phenyl)pyrazin-2-yl)-1,3,4-oxadiazol-2-yl)phenyl)-N-methylmethanaminium formate 43d (Abd131).

^{1}H NMR (400 MHz, DMSO-d_6) δ 11.04 (br, 1H), 9.00 (s, 1H), 8.30 (d, *J* = 8.6 Hz, 2H), 8.21 – 8.16 (m, 3H), 7.89 (d, *J* = 8.6 Hz, 2H), 7.83 (br, 2H), 7.70 (d, *J* = 8.3 Hz, 2H), 7.64 (d, *J* =

8.5 Hz, 2H), 7.26 (d, *J* = 2.1 Hz, 1H), 7.16 (dd, *J* = 8.7, 2.2 Hz, 1H), 5.05 (dd, *J* = 12.9, 5.4 Hz, 1H), 4.14 (s, 2H), 3.54 (s, 4H), 3.47 – 3.35 (m, 4H), 2.93 – 2.73 (m, 3H), 2.62 – 2.50 (m, 5H), 2.26 (t, *J* = 7.4 Hz, 2H), 2.04 – 1.95 (m, 1H), 1.46 – 1.34 (m, 4H), 1.30 – 1.18 (m, 2H). ^{13}C NMR (101 MHz, DMSO-d_6) δ 173.21, 171.17, 170.48, 167.92, 167.37, 164.13, 163.33, 155.21, 153.27, 144.29, 140.42, 139.85, 138.90, 138.60, 134.25, 130.84, 127.62, 127.59, 126.22, 125.31, 123.40, 120.10, 118.89, 118.11, 108.25, 52.14, 49.23, 47.19, 46.93, 44.47, 42.91, 33.47, 32.49, 31.43, 29.26, 26.22, 24.60, 22.62. HRMS (ESI, positive): Calcd. for $C_{43}H_{46}N_{11}O_8S$ $[M+H]^+$: *m/z* = 876.325; Found: 876.325. HPLC t_R = 9.92 min (purity 99.2%).

1-(4-(5-(3-Amino-6-(4-(N-(7-(4-(2-(2,6-dioxopiperidin-3-yl)-1,3-dioxoisoindolin-5-yl)piperazin-1-yl)-7-oxoheptyl)sulfamoyl)phenyl)pyrazin-2-yl)-1,3,4-oxadiazol-2-yl)phenyl)-N-methylmethanaminium formate 43e (Abd135).

^{1}H NMR (400 MHz, DMSO-d_6) δ 11.02 (br, 1H), 8.99 (s, 1H), 8.29 (d, *J* = 8.5 Hz, 2H), 8.26 (s, 1H), 8.13 (d, *J* = 8.2 Hz, 2H), 7.89 (d, *J* = 8.5 Hz, 2H), 7.83 (br, 2H), 7.65 (d, *J* = 8.5 Hz, 4H), 7.27 (d, *J* = 1.9 Hz, 1H), 7.17 (dd, *J* = 8.7, 2.1 Hz, 1H), 5.05 (dd, *J* = 12.9, 5.4 Hz, 1H), 3.95 (s, 2H), 3.54 (d, *J* = 5.4 Hz, 4H), 3.41 (d, *J* = 19.9 Hz, 4H), 2.93 – 2.80 (m, 1H), 2.77 (t, *J* = 6.7 Hz, 2H), 2.62 – 2.50 (m, 2H), 2.41 (s, 3H), 2.26 (t, *J* = 7.4 Hz, 2H), 2.05 – 1.95 (m, 1H), 1.47 – 1.31 (m, 4H), 1.27 – 1.12 (m, 4H). ^{13}C NMR (101 MHz, DMSO-d_6) δ 173.10, 171.12, 170.37, 167.81, 167.27, 164.69, 164.19, 163.12, 155.12, 153.13, 144.11, 142.08, 140.30, 139.76, 138.48, 134.14, 130.06, 127.48, 127.32, 126.10, 125.20, 122.49, 120.05, 118.78, 118.03, 108.18, 53.23, 49.13, 47.11, 46.84, 44.36, 42.85, 34.36, 32.42, 31.33, 29.21, 28.57, 26.19, 24.84, 22.52. HRMS (ESI, positive): Calcd. for $C_{44}H_{48}N_{11}O_8S$ $[M+H]^+$: *m/z* = 890.340; Found: 890.340. HPLC t_R = 10.27 min (purity 99.9%).

3-Amino-6-(4-(N-(2-(2-(3-(4-(2-(2,6-dioxopiperidin-3-yl)-1,3-dioxoisoindolin-5-yl)piperazin-1-yl)-3-oxopropoxy)ethoxy)ethyl)sulfamoyl)phenyl)-N-phenylpyrazine-2-carboxamide 43f (Abd102)

^{1}H NMR (400 MHz, DMSO-d_6) δ 11.05 (s, 1H), 10.39 (s, 1H), 8.98 (s, 1H), 8.41 (d, *J* = 8.6 Hz, 2H), 7.91 – 7.70 (m, 7H), 7.65 (d, *J* = 8.5 Hz, 1H), 7.38 (t, *J* = 7.9 Hz, 2H), 7.29 (d, *J* = 2.0 Hz, 1H), 7.21 – 7.11 (m, 2H), 5.05 (dd, *J* = 12.9, 5.4 Hz, 1H), 3.64 – 3.52 (m, 6H), 3.51 – 3.34 (m, 10H), 2.96 – 2.80 (m, 3H), 2.62 – 2.50 (m, 4H), 2.04 – 1.96 (m, 1H). ^{13}C NMR (101 MHz, DMSO-d_6) δ 173.20, 170.48, 169.47, 167.93, 167.39, 164.79, 155.23, 155.08, 145.64, 140.20, 139.82, 138.25, 137.17, 134.27, 129.05, 127.33, 126.53, 125.32, 124.75, 124.71, 121.65, 118.89, 118.13, 108.30, 70.00, 69.50, 67.12, 49.23, 47.17, 46.89, 44.57, 42.82, 40.79,

33.23, 31.43, 22.62. HRMS (ESI, positive): Calcd. for $C_{41}H_{44}N_9O_{10}S$ $[M+H]^+$: *m/z* = 854.293; Found: 854.292. HPLC t_R = 13.04 min (purity 99.8%).

3-Amino-6-(4-(N-(2-(2-(2-(3-(4-(2-(2,6-dioxopiperidin-3-yl)-1,3-dioxoisoindolin-5-yl)piperazin-1-yl)-3-oxopropoxy)ethoxy)ethoxy)ethyl)sulfamoyl)phenyl)-N-phenyl-pyrazine-2-carboxamide 43g (Abd104)

^{1}H NMR (400 MHz, DMSO-d_6) δ 11.05 (s, 1H), 10.39 (s, 1H), 8.98 (s, 1H), 8.41 (d, *J* = 8.6 Hz, 2H), 7.89 – 7.71 (m, 7H), 7.66 (d, *J* = 8.5 Hz, 1H), 7.38 (t, *J* = 7.9 Hz, 2H), 7.29 (d, *J* = 2.0 Hz, 1H), 7.21 – 7.11 (m, 2H), 5.05 (dd, *J* = 12.9, 5.4 Hz, 1H), 3.64 – 3.53 (m, 6H), 3.52 – 3.34 (m, 14H), 2.91 (q, *J* = 5.8 Hz, 2H), 2.88 – 2.80 (m, 1H), 2.62 – 2.50 (m, 4H), 2.04 – 1.96 (m, 1H). ^{13}C NMR (101 MHz, DMSO-d_6) δ 173.21, 170.48, 169.50, 167.94, 167.39, 164.79, 155.24, 155.08, 145.64, 140.20, 139.81, 138.25, 137.17, 134.27, 129.05, 127.33, 126.53, 125.32, 124.74, 124.72, 121.65, 118.89, 118.13, 108.30, 70.19, 70.09, 70.03, 69.50, 67.16, 49.24, 47.19, 46.89, 44.60, 42.81, 40.80, 33.24, 31.43, 22.62. HRMS (ESI, positive): Calcd. for $C_{43}H_{47}N_9NaO_{11}S$ $[M+Na]^+$: *m/z* = 920.301; Found: 920.302. HPLC t_R = 13.16 min (purity 98.8%).

3-Amino-6-(4-(N-(6-(4-(2-(2,6-dioxopiperidin-3-yl)-1,3-dioxoisoindolin-5-yl)piperazin-1-yl)-6-oxohexyl)sulfamoyl)phenyl)-N-phenylpyrazine-2-carboxamide 43h (Abd107).

^{1}H NMR (400 MHz, DMSO-d_6) δ 11.05 (s, 1H), 10.39 (s, 1H), 8.98 (s, 1H), 8.42 (d, *J* = 8.5 Hz, 2H), 7.92 – 7.72 (m, 6H), 7.69 – 7.58 (m, 2H), 7.38 (t, *J* = 7.9 Hz, 2H), 7.29 (d, *J* = 1.9 Hz, 1H), 7.23 – 7.09 (m, 2H), 5.05 (dd, *J* = 12.9, 5.4 Hz, 1H), 3.54 (s, 4H), 3.42 (d, *J* = 16.1 Hz, 4H), 2.93 – 2.79 (m, 1H), 2.75 (dd, *J* = 12.9, 6.7 Hz, 2H), 2.63 – 2.51 (m, 2H), 2.26 (t, *J* = 7.3 Hz, 2H), 2.04 – 1.93 (m, 1H), 1.49 – 1.32 (m, 4H), 1.30 – 1.17 (m, 2H). ^{13}C NMR (101 MHz, DMSO-d_6) δ 173.21, 171.17, 170.48, 167.94, 167.39, 164.80, 155.25, 155.08, 145.64, 140.18, 139.77, 138.25, 137.16, 134.27, 129.05, 127.32, 126.56, 125.34, 124.75, 124.72, 121.67, 118.91, 108.31, 49.24, 47.21, 46.95, 44.47, 42.91, 32.49, 31.42, 29.27, 26.24, 24.60, 22.62. HRMS (ESI, positive): Calcd. for $C_{40}H_{42}N_9O_8S$ $[M+H]^+$: *m/z* = 808.287; Found: 808.288. HPLC t_R = 13.24 min (purity 98.3%).

3-Amino-6-(4-(N-(7-(4-(2-(2,6-dioxopiperidin-3-yl)-1,3-dioxoisoindolin-5-yl)piperazin-1-yl)-7-oxoheptyl)sulfamoyl)phenyl)-N-phenylpyrazine-2-carboxamide 43i (Abd125).

^{1}H NMR (400 MHz, DMSO-d_6) δ 11.05 (s, 1H), 10.39 (s, 1H), 8.98 (s, 1H), 8.42 (d, *J* = 8.5 Hz, 2H), 7.93 – 7.72 (m, 6H), 7.66 (d, *J* = 8.5 Hz, 1H), 7.61 (t, *J* = 5.7 Hz, 1H), 7.38 (t, *J* =

7.9 Hz, 2H), 7.30 (d, *J* = 1.9 Hz, 1H), 7.23 – 7.10 (m, 2H), 5.05 (dd, *J* = 12.9, 5.4 Hz, 1H), 3.55 (s, 4H), 3.43 (d, *J* = 19.3 Hz, 4H), 2.93 – 2.80 (m, 1H), 2.75 (dd, *J* = 13.0, 6.7 Hz, 2H), 2.61 – 2.50 (m, 2H), 2.26 (t, *J* = 7.4 Hz, 2H), 2.04 – 1.95 (m, 1H), 1.47 – 1.31 (m, 4H), 1.26 – 1.13 (m, 4H). ^{13}C NMR (101 MHz, DMSO-d_6) δ 173.20, 171.23, 170.48, 167.94, 167.39, 164.80, 155.26, 155.08, 145.64, 140.20, 139.77, 138.25, 137.16, 134.27, 129.05, 127.32, 126.55, 125.33, 124.75, 121.66, 118.91, 118.16, 108.33, 55.34, 49.24, 47.22, 46.96, 44.47, 42.95, 32.53, 31.43, 29.29, 28.68, 26.31, 24.95, 22.62. HRMS (ESI, positive): Calcd. for $C_{41}H_{44}N_9O_8S$ $[M+H]^+$: *m/z* = 822.303; Found: 822.303. HPLC t_R = 13.61 min (purity 98.7%).

3-Amino-6-(4-(N-(5-(4-(2-(2,6-dioxopiperidin-3-yl)-1,3-dioxoisoindolin-5-yl)piperazin-1-yl)-5-oxopentyl)sulfamoyl)phenyl)-N-phenylpyrazine-2-carboxamide 43j (Abd128).

^{1}H NMR (400 MHz, DMSO-d_6) δ 11.05 (s, 1H), 10.38 (s, 1H), 8.98 (s, 1H), 8.42 (d, *J* = 8.5 Hz, 2H), 7.91 – 7.73 (m, 6H), 7.64 (dd, *J* = 10.1, 4.3 Hz, 2H), 7.38 (t, *J* = 7.9 Hz, 2H), 7.28 (d, *J* = 1.9 Hz, 1H), 7.20 – 7.11 (m, 2H), 5.05 (dd, *J* = 12.9, 5.4 Hz, 1H), 3.54 (s, 4H), 3.41 (d, *J* = 18.3 Hz, 4H), 2.92 – 2.74 (m, 3H), 2.61 – 2.50 (m, 2H), 2.26 (t, *J* = 7.0 Hz, 2H), 2.04 – 1.95 (m, 1H), 1.52 – 1.37 (m, 4H). ^{13}C NMR (101 MHz, DMSO-d_6) δ 173.21, 171.05, 170.49, 167.93, 167.38, 164.78, 155.22, 155.07, 145.63, 140.17, 139.77, 138.24, 137.14, 134.26, 129.04, 127.33, 126.55, 125.32, 124.73, 121.66, 118.92, 118.11, 108.29, 55.33, 49.23, 47.19, 46.93, 44.46, 42.82, 32.03, 31.42, 29.06, 22.62, 22.22. HRMS (ESI, positive): Calcd. for $C_{39}H_{39}N_9NaO_8S$ $[M+Na]^+$: *m/z* = 816.254; Found: 816.254. HPLC t_R = 13.17 min (purity 97.7%).

3-Amino-6-(4-(N-(8-(4-(2-(2,6-dioxopiperidin-3-yl)-1,3-dioxoisoindolin-5-yl)piperazin-1-yl)-8-oxooctyl)sulfamoyl)phenyl)-N-phenylpyrazine-2-carboxamide 43k (Abd137).

^{1}H NMR (400 MHz, DMSO-d_6) δ 11.05 (s, 1H), 10.40 (s, 1H), 8.98 (s, 1H), 8.42 (d, *J* = 8.5 Hz, 2H), 7.91 – 7.73 (m, 6H), 7.67 (d, *J* = 8.5 Hz, 1H), 7.61 (t, *J* = 5.7 Hz, 1H), 7.38 (t, *J* = 7.9 Hz, 2H), 7.30 (d, *J* = 1.9 Hz, 1H), 7.23 – 7.11 (m, 2H), 5.05 (dd, *J* = 12.9, 5.4 Hz, 1H), 3.55 (s, 4H), 3.43 (d, *J* = 18.2 Hz, 4H), 2.92 – 2.82 (m, 1H), 2.75 (dd, *J* = 12.9, 6.7 Hz, 2H), 2.62 – 2.51 (m, 2H), 2.26 (t, *J* = 7.4 Hz, 2H), 2.04 – 1.96 (m, 1H), 1.48 – 1.30 (m, 4H), 1.25 – 1.13 (m, 6H). ^{13}C NMR (101 MHz, DMSO-d_6) δ 173.21, 171.26, 170.48, 167.94, 167.39, 164.80, 155.27, 155.08, 145.63, 140.22, 139.76, 138.25, 137.17, 134.27, 129.05, 127.32, 126.54, 125.34, 124.74, 121.66, 118.90, 118.16, 108.33, 49.24, 47.22, 46.96, 44.49, 42.96, 32.60, 31.43, 29.35, 29.08, 28.80, 26.37, 25.00, 22.63. HRMS (ESI, positive): Calcd. for $C_{42}H_{46}N_9O_8S$ $[M+H]^+$: *m/z* = 836.318; Found: 836.320. HPLC t_R = 14.36 min (purity 96.4%).

3-Amino-6-(4-(N-(7-((2-(4-(2,6-dioxopiperidin-3-yl)phenoxy)ethyl)amino)-7-oxoheptyl)sulfamoyl)phenyl)-N-phenylpyrazine-2-carboxamide 44a (Abd126).

^{1}H NMR (400 MHz, DMSO-d_6) δ 10.75 (s, 1H), 10.40 (s, 1H), 8.98 (s, 1H), 8.42 (d, *J* = 8.5 Hz, 2H), 7.95 (t, *J* = 5.4 Hz, 1H), 7.90 – 7.72 (m, 6H), 7.59 (t, *J* = 5.8 Hz, 1H), 7.38 (t, *J* = 7.9 Hz, 2H), 7.15 (t, *J* = 7.4 Hz, 1H), 7.09 (d, *J* = 8.6 Hz, 2H), 6.85 (d, *J* = 8.6 Hz, 2H), 3.91 (t, *J* = 5.7 Hz, 2H), 3.75 (dd, *J* = 11.3, 4.9 Hz, 1H), 3.35 (dd, *J* = 11.2, 5.6 Hz, 2H), 2.72 (dd, *J* = 13.0, 6.7 Hz, 2H), 2.67 – 2.56 (m, 1H), 2.46 – 2.40 (m, 1H), 2.18 – 2.07 (m, 1H), 2.05 – 1.93 (m, 3H), 1.46 – 1.27 (m, 4H), 1.25 – 1.09 (m, 4H). ^{13}C NMR (101 MHz, DMSO-d_6) δ 174.85, 173.84, 172.84, 164.82, 157.75, 155.09, 145.64, 140.16, 139.77, 138.27, 137.18, 131.61, 129.98, 129.05, 127.31, 126.56, 124.76, 124.72, 121.67, 114.74, 66.76, 46.93, 42.98, 38.57, 35.61, 31.78, 29.29, 28.57, 26.43, 26.25, 25.53. HRMS (ESI, positive): Calcd. for $C_{37}H_{41}N_7NaO_7S$ $[M+Na]^+$: *m/z* = 750.269; Found: 750.270. HPLC t_R = 13.34 min (purity 97.6%).

3-Amino-6-(4-(N-(5-((2-(4-(2,6-dioxopiperidin-3-yl)phenoxy)ethyl)amino)-5-oxopentyl)sulfamoyl)phenyl)-N-phenylpyrazine-2-carboxamide 44b (Abd129).

^{1}H NMR (400 MHz, DMSO-d_6) δ 10.75 (s, 1H), 10.41 (s, 1H), 8.98 (s, 1H), 8.42 (d, *J* = 8.5 Hz, 2H), 7.97 (t, *J* = 5.5 Hz, 1H), 7.90 – 7.72 (m, 6H), 7.62 (t, *J* = 5.8 Hz, 1H), 7.38 (t, *J* = 7.9 Hz, 2H), 7.15 (t, *J* = 7.4 Hz, 1H), 7.09 (d, *J* = 8.6 Hz, 2H), 6.85 (d, *J* = 8.6 Hz, 2H), 3.91 (t, *J* = 5.7 Hz, 2H), 3.75 (dd, *J* = 11.3, 4.9 Hz, 1H), 3.35 (dd, *J* = 11.3, 5.7 Hz, 2H), 2.73 (dd, *J* = 13.0, 6.6 Hz, 2H), 2.65 – 2.57 (m, 1H), 2.47 – 2.39 (m, 1H), 2.17 – 2.06 (m, 1H), 2.06 – 1.92 (m, 3H), 1.51 – 1.41 (m, 2H), 1.40 – 1.29 (m, 2H). ^{13}C NMR (101 MHz, DMSO-d_6) δ 174.85, 173.84, 172.60, 164.82, 157.73, 155.09, 145.65, 140.12, 139.77, 138.27, 137.19, 131.62, 129.98, 129.06, 127.31, 126.57, 124.76, 124.73, 121.67, 114.75, 66.75, 46.93, 42.81, 38.57, 35.11, 31.78, 29.11, 26.42, 22.83. HRMS (ESI, positive): Calcd. for $C_{35}H_{38}N_7O_7S$ $[M+H]^+$: *m/z* = 700.255; Found: 700.255. HPLC t_R = 13.18 min (purity 99.7%).

3-Amino-6-(4-(N-(8-((2-(4-(2,6-dioxopiperidin-3-yl)phenoxy)ethyl)amino)-8-oxooctyl)sulfamoyl)phenyl)-N-phenylpyrazine-2-carboxamide 44c (Abd138).

^{1}H NMR (400 MHz, DMSO-d_6) δ 10.76 (s, 1H), 10.41 (s, 1H), 8.98 (s, 1H), 8.42 (d, *J* = 8.6 Hz, 2H), 7.95 (t, *J* = 5.4 Hz, 1H), 7.90 – 7.74 (m, 6H), 7.60 (t, *J* = 5.8 Hz, 1H), 7.41 – 7.35 (m, 2H), 7.18 – 7.12 (m, 1H), 7.09 (d, *J* = 8.7 Hz, 2H), 6.86 (d, *J* = 8.7 Hz, 2H), 3.92 (t, *J* = 5.7 Hz, 2H), 3.75 (dd, *J* = 11.3, 4.9 Hz, 1H), 3.36 (q, *J* = 5.6 Hz, 2H), 2.72 (dd, *J* = 13.0, 6.8

Hz, 2H), 2.68 – 2.56 (m, 1H), 2.47 – 2.39 (m, 1H), 2.18 – 2.06 (m, 1H), 2.05 – 1.91 (m, 3H), 1.49 – 1.38 (m, 2H), 1.37 – 1.29 (m, 2H), 1.23 – 1.10 (m, 6H). ^{13}C NMR (101 MHz, DMSO-d_6) δ 174.84, 173.84, 172.87, 164.82, 157.76, 155.09, 145.63, 140.18, 139.77, 138.27, 137.18, 131.61, 129.98, 129.05, 127.31, 126.55, 124.76, 124.72, 121.67, 114.74, 66.77, 46.93, 42.99, 38.58, 35.68, 31.78, 29.42, 28.94, 28.73, 26.44, 26.38, 25.57. HRMS (ESI, positive): Calcd. for $C_{38}H_{44}N_7O_7S$ $[M+H]^+$: *m/z* = 742.302; Found: 742.302. HPLC t_R = 14.05 min (purity 98.4%).

3-Amino-6-(4-(N-(6-(4-(6-((2,6-dioxopiperidin-3-yl)carbamoyl)pyridin-2-yl)piperazin-1-yl)-6-oxohexyl)sulfamoyl)phenyl)-N-phenylpyrazine-2-carboxamide 44d (Abd106).

^{1}H NMR (400 MHz, DMSO-d_6) δ 10.86 (s, 1H), 10.40 (s, 1H), 8.98 (s, 1H), 8.75 (d, *J* = 8.4 Hz, 1H), 8.42 (d, *J* = 8.3 Hz, 2H), 7.93 – 7.54 (m, 8H), 7.38 (t, *J* = 7.7 Hz, 2H), 7.32 (d, *J* = 7.2 Hz, 1H), 7.15 (t, *J* = 7.3 Hz, 1H), 7.01 (d, *J* = 8.6 Hz, 1H), 4.78 – 4.66 (m, 1H), 3.67 – 3.41 (m, 8H), 2.87 – 2.66 (m, 3H), 2.58 – 2.50 (m, 1H), 2.35 – 2.15 (m, 3H), 1.97 (dd, *J* = 8.5, 3.4 Hz, 1H), 1.49 – 1.33 (m, 4H), 1.31 – 1.19 (m, 2H). ^{13}C NMR (101 MHz, DMSO-d_6) δ 173.44, 172.69, 171.12, 164.81, 164.58, 158.00, 155.08, 147.89, 145.64, 140.15, 139.78, 139.28, 138.26, 137.17, 129.05, 127.32, 126.57, 124.76, 124.72, 121.68, 111.79, 110.78, 49.88, 45.11, 44.92, 44.72, 42.92, 41.05, 32.57, 31.46, 29.32, 26.29, 24.71, 24.49. HRMS (ESI, positive): Calcd. for $C_{38}H_{43}N_{10}O_7S$ $[M+H]^+$: *m/z* = 783.3031; Found: 783.3027. HPLC t_R = 13.23 min (purity 95.2%).

3-Amino-6-(4-(N-(2-(2-(3-(((S)-1-((2S,4R)-4-hydroxy-2-((4-(4-methylthiazol-5-yl)benzyl)carbamoyl)pyrrolidin-1-yl)-3,3-dimethyl-1-oxobutan-2-yl)amino)-3-oxoprop-oxy)ethoxy)ethyl)sulfamoyl)phenyl)-N-phenylpyrazine-2-carboxamide 45a (Abd101).

^{1}H NMR (400 MHz, DMSO-d_6) δ 10.41 (s, 1H), 8.98 (s, 1H), 8.95 (s, 1H), 8.52 (t, *J* = 6.0 Hz, 1H), 8.41 (d, *J* = 8.5 Hz, 2H), 7.92 – 7.71 (m, 8H), 7.45 – 7.32 (m, 6H), 7.14 (t, *J* = 7.4 Hz, 1H), 5.09 (d, *J* = 3.5 Hz, 1H), 4.52 (d, *J* = 9.4 Hz, 1H), 4.46 – 4.28 (m, 3H), 4.20 (dd, *J* = 15.8, 5.5 Hz, 1H), 3.68 – 3.50 (m, 4H), 3.48 – 3.34 (m, 6H), 2.91 (dd, *J* = 11.7, 5.8 Hz, 2H), 2.56 – 2.49 (m, 1H), 2.42 (s, 3H), 2.36 – 2.25 (m, 1H), 2.07 – 1.95 (m, 1H), 1.93 – 1.83 (m, 1H), 0.89 (s, 9H). ^{13}C NMR (101 MHz, DMSO-d_6) δ 172.32, 170.35, 169.96, 164.81, 155.09, 151.84, 148.15, 145.64, 140.17, 139.92, 139.83, 138.26, 137.19, 131.59, 130.09, 129.07, 129.05, 127.86, 127.33, 126.54, 124.77, 124.72, 121.68, 69.98, 69.78, 69.54, 69.31, 67.35, 59.14, 56.73, 42.79, 42.10, 38.38, 36.08, 35.78, 26.75, 16.38. HRMS (ESI, positive): Calcd.

for $C_{46}H_{55}N_9NaO_9S_2$ $[M+Na]^+$: *m/z* = 964.346 ; Found: 964.347. HPLC t_R = 14.39 min (purity 100%).

3-Amino-6-(4-(N-((S)-14-((2S,4R)-4-hydroxy-2-((4-(4-methylthiazol-5-yl)benzyl)carbamoyl)pyrrolidine-1-carbonyl)-15,15-dimethyl-12-oxo-3,6,9-trioxa-13-azahexadecyl)sulfamoyl)phenyl)-N-phenylpyrazine-2-carboxamide 45b (Abd103).

^{1}H NMR (400 MHz, DMSO-d_6) δ 10.40 (s, 1H), 8.98 (s, 1H), 8.95 (s, 1H), 8.52 (t, *J* = 5.9 Hz, 1H), 8.41 (d, *J* = 8.6 Hz, 2H), 7.91 – 7.72 (m, 8H), 7.44 – 7.33 (m, 6H), 7.14 (t, *J* = 7.4 Hz, 1H), 5.09 (br, 1H), 4.53 (d, *J* = 9.4 Hz, 1H), 4.46 – 4.28 (m, 3H), 4.20 (dd, *J* = 15.8, 5.4 Hz, 1H), 3.69 – 3.51 (m, 4H), 3.49 – 3.37 (m, 10H), 2.91 (q, *J* = 5.8 Hz, 2H), 2.55 – 2.49 (m, 1H), 2.42 (s, 3H), 2.36 – 2.27 (m, 1H), 2.06 – 1.97 (m, 1H), 1.93 – 1.83 (m, 1H), 0.90 (s, 9H). ^{13}C NMR (101 MHz, DMSO-d_6) δ 172.33, 170.35, 169.97, 164.81, 155.09, 151.84, 148.15, 145.64, 140.19, 139.93, 139.82, 138.27, 137.19, 131.59, 130.08, 129.07, 129.05, 127.86, 127.33, 126.55, 124.77, 124.72, 121.67, 70.13, 70.10, 70.03, 69.89, 69.54, 69.31, 67.37, 59.15, 56.80, 56.74, 42.80, 42.10, 38.38, 36.10, 35.79, 26.76, 16.37. HRMS (ESI, positive): Calcd. for $C_{48}H_{59}N_9NaO_{10}S_2$ $[M+Na]^+$: *m/z* = 1008.372; Found: 1008.374. HPLC t_R = 14.43 min (purity 99.6%).

3-Amino-6-(4-(N-(6-(((S)-1-((2S,4R)-4-hydroxy-2-((4-(4-methylthiazol-5-yl)benzyl)carbamoyl)pyrrolidin-1-yl)-3,3-dimethyl-1-oxobutan-2-yl)amino)-6-oxohexyl)sulfamoyl)phenyl)-N-phenylpyrazine-2-carboxamide 45c (Abd105).

^{1}H NMR (400 MHz, DMSO-d_6) δ 10.41 (s, 1H), 8.98 (s, 1H), 8.95 (s, 1H), 8.51 (t, *J* = 6.0 Hz, 1H), 8.42 (d, *J* = 8.5 Hz, 2H), 7.89 – 7.73 (m, 7H), 7.60 (t, *J* = 5.7 Hz, 1H), 7.43 – 7.31 (m, 6H), 7.14 (t, *J* = 7.4 Hz, 1H), 5.08 (d, *J* = 3.5 Hz, 1H), 4.50 (d, *J* = 9.4 Hz, 1H), 4.46 – 4.29 (m, 3H), 4.19 (dd, *J* = 15.8, 5.4 Hz, 1H), 3.68 – 3.56 (m, 2H), 2.72 (dd, *J* = 13.0, 6.8 Hz, 2H), 2.42 (s, 3H), 2.27 – 2.14 (m, 1H), 2.12 – 1.96 (m, 2H), 1.93 – 1.83 (m, 1H), 1.46 – 1.31 (m, 4H), 1.26 – 1.16 (m, 2H), 0.89 (s, 9H). ^{13}C NMR (101 MHz, DMSO-d_6) δ 172.38, 172.35, 170.13, 164.82, 155.09, 151.85, 148.15, 145.64, 140.10, 139.93, 139.77, 138.27, 137.18, 131.59, 130.08, 129.06, 129.05, 127.86, 127.32, 126.56, 124.77, 124.71, 121.67, 69.30, 59.12, 56.73, 42.94, 42.10, 38.38, 35.63, 35.20, 29.24, 26.81, 26.27, 25.43, 16.38. HRMS (ESI, positive): Calcd. for $C_{45}H_{54}N_9O_7S_2$ $[M+H]^+$: *m/z* = 896.358; Found: 896.358. HPLC t_R = 14.46 min (purity 97.9%).

(2S,4R)-1-((S)-2-(6-((4-(5-amino-6-(5-(4-((methylamino)methyl)phenyl)-1,3,4-oxadiazol-2-yl)pyrazin-2-yl)phenyl)sulfonamido)hexanamido)-3,3-dimethylbutanoyl)-4-hydroxy-N-(4-(4-methylthiazol-5-yl)benzyl)pyrrolidine-2-carboxamide 45d (Abd112).

^{1}H NMR (400 MHz, DMSO-d_6) δ 8.99 (s, 1H), 8.95 (s, 1H), 8.52 (t, *J* = 5.9 Hz, 1H), 8.29 (d, *J* = 8.5 Hz, 2H), 8.10 (d, *J* = 8.2 Hz, 2H), 7.95 – 7.73 (m, 5H), 7.61 (d, *J* = 8.2 Hz, 3H), 7.37 (q, *J* = 8.2 Hz, 4H), 5.09 (br, 1H), 4.50 (d, *J* = 9.4 Hz, 1H), 4.46 – 4.28 (m, 3H), 4.19 (dd, *J* = 15.9, 5.3 Hz, 1H), 3.80 (s, 2H), 3.67 – 3.55 (m, 2H), 2.78 – 2.69 (m, 2H), 2.41 (s, 3H), 2.32 (s, 3H), 2.23 – 2.14 (m, 1H), 2.11 – 1.97 (m, 2H), 1.92 – 1.83 (m, 1H), 1.48 – 1.32 (m, 4H), 1.25 – 1.16 (m, 2H), 0.89 (s, 9H). ^{13}C NMR (101 MHz, DMSO-d_6) δ 172.40, 172.35, 170.13, 164.45, 163.17, 153.24, 151.83, 148.14, 144.17, 140.30, 139.92, 139.88, 138.60, 131.58, 130.07, 129.57, 129.05, 127.85, 127.58, 127.31, 126.21, 121.97, 120.23, 69.30, 59.12, 56.74, 54.60, 42.94, 42.10, 38.37, 35.62, 35.59, 35.21, 29.26, 26.81, 26.26, 25.44, 16.37. HRMS (ESI, positive): Calcd. for $C_{48}H_{58}N_{11}O_7S_2$ $[M+H]^+$: *m/z* = 964.396; Found: 964.395. HPLC t_R = 13.37 min (purity 98.1%).

(2S,4R)-1-((S)-2-(6-((4-(5-amino-6-(5-phenyl-1,3,4-oxadiazol-2-yl)pyrazin-2-yl)phenyl)sulfonamido)hexanamido)-3,3-dimethylbutanoyl)-4-hydroxy-N-(4-(4-methylthiazol-5-yl)benzyl)pyrrolidine-2-carboxamide 45e (Abd115).

^{1}H NMR (400 MHz, DMSO-d_6) δ 8.99 (s, 1H), 8.95 (s, 1H), 8.51 (t, *J* = 5.9 Hz, 1H), 8.29 (d, *J* = 8.5 Hz, 2H), 8.15 (dd, *J* = 7.6, 1.7 Hz, 2H), 7.95 – 7.73 (m, 5H), 7.70 – 7.56 (m, 4H), 7.37 (q, *J* = 8.3 Hz, 4H), 5.08 (d, *J* = 3.5 Hz, 1H), 4.50 (d, *J* = 9.4 Hz, 1H), 4.45 – 4.28 (m, 3H), 4.19 (dd, *J* = 15.8, 5.2 Hz, 1H), 3.67 – 3.55 (m, 2H), 2.74 (dd, *J* = 13.0, 6.7 Hz, 2H), 2.41 (s, 3H), 2.24 – 2.14 (m, 1H), 2.11 – 1.96 (m, 2H), 1.92 – 1.83 (m, 1H), 1.45 – 1.32 (m, 4H), 1.25 – 1.16 (m, 2H), 0.89 (s, 9H). ^{13}C NMR (101 MHz, DMSO-d_6) δ 172.39, 172.35, 170.13, 164.43, 163.29, 153.25, 151.84, 148.14, 144.22, 140.31, 139.92, 139.88, 138.61, 132.86, 131.58, 130.07, 129.99, 129.05, 127.85, 127.58, 127.40, 126.21, 123.48, 120.20, 69.30, 59.12, 56.73, 42.94, 42.10, 38.37, 35.62, 35.21, 29.25, 26.80, 26.25, 25.43, 16.37. HRMS (ESI, positive): Calcd. for $C_{46}H_{53}N_{10}O_7S_2$ $[M+H]^+$: *m/z* = 921.353; Found: 921.354. HPLC t_R = 14.75 min (purity 99.6%).

(2S,4R)-1-((S)-2-(5-((4-(5-amino-6-(5-phenyl-1,3,4-oxadiazol-2-yl)pyrazin-2-yl)phenyl)sulfonamido)pentanamido)-3,3-dimethylbutanoyl)-4-hydroxy-N-(4-(4-methylthiazol-5-yl)benzyl)pyrrolidine-2-carboxamide 45f (Abd119).

^{1}H NMR (400 MHz, DMSO-d_6) δ 8.99 (s, 1H), 8.94 (s, 1H), 8.51 (t, *J* = 5.9 Hz, 1H), 8.29 (d, *J* = 8.5 Hz, 2H), 8.19 – 8.10 (m, 2H), 7.93 – 7.74 (m, 5H), 7.70 – 7.59 (m, 4H), 7.36 (q, *J* = 8.3 Hz, 4H), 5.08 (d, *J* = 3.5 Hz, 1H), 4.50 (d, *J* = 9.3 Hz, 1H), 4.44 – 4.29 (m, 3H), 4.19 (dd, *J* = 15.9, 5.4 Hz, 1H), 3.69 – 3.56 (m, 2H), 2.76 (dd, *J* = 12.6, 6.4 Hz, 2H), 2.41 (s, 3H), 2.26 – 2.13 (m, 1H), 2.13 – 1.96 (m, 2H), 1.92 – 1.83 (m, 1H), 1.51 – 1.32 (m, 4H), 0.89 (s, 9H). ^{13}C NMR (101 MHz, DMSO-d_6) δ 172.35, 172.23, 170.11, 164.42, 163.28, 153.25, 151.83, 148.14, 144.21, 140.36, 139.91, 139.87, 138.61, 132.85, 131.58, 130.07, 129.98, 129.05, 127.84, 127.56, 127.39, 126.20, 123.47, 120.19, 69.30, 59.12, 56.75, 42.84, 42.10, 38.37, 35.63, 34.81, 29.25, 26.81, 23.11, 16.37. HRMS (ESI, positive): Calcd. for $C_{45}H_{50}N_{10}NaO_7S_2$ $[M+Na]^+$: *m/z* = 929.320; Found: 929.320. HPLC t_R = 14.61 min (purity 99.8%).

4.4. Non-enzymatic stability testing

The developed compounds were diluted in the assay media consisting of a mixture of DMEM (50%), DMSO (10%) and acetonitrile (40%) at pH 7.4 and incubated at 37°C for 72 h. The quantity of the compounds was measured after 6, 12, 24, 48, and 72 h by HPLC using an XTerra RP18 column (3.5 mm, 3.9 mm × 100 mm) from the manufacturer Waters (Milford, MA, USA) and two LC-10AD pumps, an SPD-M10AVP PDA detector, and an SIL-HT autosampler, all from the manufacturer Shimadzu (Kyoto, Japan)

4.5. Cellular assay / degradation assay

4.5.1 Drugs and chemicals used as references

Bortezomib (#S1013), MG132 (#S2619), and VE-821 (#S8007) were purchased from Selleck Chemicals, Munich, Germany. Irinotecan (#I1406) was purchased from Sigma-Aldrich, Taufkirchen, Germany. Stock solutions in DMSO were stored at -80 °C. All drugs were diluted in PBS before treatment.

4.5.2 Cell lines

Human pancreatic cancer cell line MIA PaCa-2 was kindly provided by Matthias Wirth (Berlin, Germany). The human cervix cancer cell line HeLa was a gift from Roland H. Stauber (Mainz, Germany). Cells were cultured in high glucose Dulbecco′s Modified Eagle′s Medium (DMEM; D5796, Sigma-Aldrich, Munich, Germany), supplemented with 10% fetal

calf serum (FCS) and 1% (w/v) penicillin/streptomycin (Thermo Fisher, Gibco, Braunschweig, Germany). Cells were confirmed to be mycoplasma-free and were verified by DNA fingerprint at the DSMZ, Braunschweig, Germany.

4.5.3 Immunoblot

Immunoblots were carried out as described by our group [34]. Antibodies used for this assay were: ATR (#cs2790), p-CHK1 (S345) (#cs2348), and CRBN (cs71810) from Cell Signaling, Leiden, Netherlands; GSPT1 (#sc-515615), HSP90 (#sc-13119), and vinculin (#sc-73614) from Santa Cruz Biotechnology, Heidelberg, Germany; ATM (#ab32420) and DNA-PKcs (#ab32566) from Abcam, Cambridge, U.K.; p-ATR (T1989) (#GTX128145) from GeneTex, CA, USA; ubiquitin (#05-1307) from Sigma-Aldrich, Taufkirchen, Germany. HSP90 and vinculin served as independent housekeeping proteins to normalize protein loading. The protein ladder used was the PageRuler^{TM} Plus pre-stained protein ladder (#26619) from Thermo Fischer Scientific, MA, USA.

4.5.4 RNA interference

Knock-down of CRBN in MIA PaCa-2 cells was performed by transfecting 30 pmol of siRNA against CRBN (Thermo Fischer Scientific, MA, USA, #4392420) or the same amount of non-targeting control siRNA-C (Santa Cruz Biotechnology, Heidelberg, Germany, #sc-44231) with Lipofectamine® RNAiMAX (Invitrogen, Darmstadt, Germany), according to manufacturer's protocol. After 48 h, growth media with transfection mixture was removed and cells were treated with Abd110 (2 µM) and/or irinotecan (5 µM) for 24 h. Knock-down efficiency was confirmed by immunoblotting

4.5.5 Cytotoxicity

To determine the cytotoxicity on the human epithelial kidney, the cell line HEK293 was used. HEK293 cells (DSMZ Braunschweig, ACC305) were incubated at 37 °C in a humidified incubator with 5% CO_2 in Dulbecco's Modified Eagle Medium (DMEM) supplemented with 10% FCS and 5 mM glutamine. Cells were seeded out at 1.5 x 10^3 cells per well in a 96-well cell culture plate (TPP, Switzerland). The compounds to be tested were added immediately to the medium at 50 µM. After 24 h, Alamar Blue reagent (Invitrogen, CA) was added and incubated again for 21 h before samples were analyzed. Detection of viable cells which convert the resazurine reagent into the highly fluorescent resorufin was performed by using a FLUOstarOPTIMA microplate reader (BMG Labtec) using the following filter set: Ex 530

nm/Em 590 nm. All measurements were performed in triplicate and data are means with standard deviation <12%.

Conflict of interest

None

Funding

This work was funded by the Deutsche Forschungsgemeinschaft (DFG) project number 528202295 (to W.S and O.H.K).

Author Contributions

A.M.A. synthesized the compounds and wrote the manuscript. R.A. and A.K. carried out all biological experiments and wrote part of the manuscript. F.E. carried out the cytotoxicity testing on human HEK293 cells. M.S. performed the purity and stability tests. O.H.K., and W.S. designed experiments, analyzed data, and revised the manuscript. O.H.K. and W.S. initiated the project and finalized the manuscript. All authors have given approval to the final version of the manuscript.

References:

[1] T. Nikolova, N. Kiweler, O.H. Krämer, Interstrand crosslink repair as a target for HDAC inhibition, Trends in pharmacological sciences, 38 (2017) 822-836.
[2] N.Y. Ngoi, M.M. Pham, D.S. Tan, T.A. Yap, Targeting the replication stress response through synthetic lethal strategies in cancer medicine, Trends in cancer, 7 (2021) 930-957.
[3] O.L. Kantidze, A.K. Velichko, A.V. Luzhin, N.V. Petrova, S.V. Razin, Synthetically lethal interactions of ATM, ATR, and DNA-PKcs, Trends in cancer, 4 (2018) 755-768.
[4] J.S. Baxter, D. Zatreanu, S.J. Pettitt, C.J. Lord, Resistance to DNA repair inhibitors in cancer, Mol. Oncol., 16 (2022) 3811-3827.
[5] A.A.B. da Costa, D. Chowdhury, G.I. Shapiro, A.D. D'Andrea, P.A. Konstantinopoulos, Targeting replication stress in cancer therapy, Nature Reviews Drug Discovery, 22 (2023) 38-58.
[6] E. Lecona, O. Fernandez-Capetillo, Targeting ATR in cancer, Nature Reviews Cancer, 18 (2018) 586-595.
[7] P.M. Reaper, M.R. Griffiths, J.M. Long, J.-D. Charrier, S. MacCormick, P.A. Charlton, J.M. Golec, J.R. Pollard, Selective killing of ATM-or p53-deficient cancer cells through inhibition of ATR, Nat. Chem. Biol., 7 (2011) 428-430.
[8] J.-D. Charrier, S.J. Durrant, J.M.C. Golec, D.P. Kay, R.M.A. Knegtel, S. MacCormick, M. Mortimore, M.E. O'Donnell, J.L. Pinder, P.M. Reaper, A.P. Rutherford, P.S.H. Wang, S.C. Young, J.R. Pollard, Discovery of Potent and Selective Inhibitors of Ataxia

Telangiectasia Mutated and Rad3 Related (ATR) Protein Kinase as Potential Anticancer Agents, J. Med. Chem., 54 (2011) 2320-2330.
[9] R. Prevo, E. Fokas, P.M. Reaper, P.A. Charlton, J.R. Pollard, W.G. McKenna, R.J. Muschel, T.B. Brunner, The novel ATR inhibitor VE-821 increases sensitivity of pancreatic cancer cells to radiation and chemotherapy, Cancer Biol. Ther., 13 (2012) 1072-1081.
[10] R. Jossé, S.E. Martin, R. Guha, P. Ormanoglu, T.D. Pfister, P.M. Reaper, C.S. Barnes, J. Jones, P. Charlton, J.R. Pollard, J. Morris, J.H. Doroshow, Y. Pommier, ATR Inhibitors VE-821 and VX-970 Sensitize Cancer Cells to Topoisomerase I Inhibitors by Disabling DNA Replication Initiation and Fork Elongation Responses, Cancer Res., 74 (2014) 6968-6979.
[11] C.J. Huntoon, K.S. Flatten, A.E. Wahner Hendrickson, A.M. Huehls, S.L. Sutor, S.H. Kaufmann, L.M. Karnitz, ATR inhibition broadly sensitizes ovarian cancer cells to chemotherapy independent of BRCA status, Cancer Res., 73 (2013) 3683-3691.
[12] R. Knegtel, J.-D. Charrier, S. Durrant, C. Davis, M. O'Donnell, P. Storck, S. MacCormick, D. Kay, J. Pinder, A. Virani, Rational design of 5-(4-(Isopropylsulfonyl) phenyl)-3-(3-(4-((methylamino) methyl) phenyl) isoxazol-5-yl) pyrazin-2-amine (VX-970, M6620): optimization of intra-and intermolecular polar interactions of a new ataxia telangiectasia mutated and Rad3-related (ATR) kinase inhibitor, J. Med. Chem., 62 (2019) 5547-5561.
[13] A. Thomas, C.E. Redon, L. Sciuto, E. Padiernos, J. Ji, M.-J. Lee, A. Yuno, S. Lee, Y. Zhang, L. Tran, Phase I study of ATR inhibitor M6620 in combination with topotecan in patients with advanced solid tumors, J. Clin. Oncol., 36 (2018) 1594.
[14] L. Gorecki, M. Andrs, M. Rezacova, J. Korabecny, Discovery of ATR kinase inhibitor berzosertib (VX-970, M6620): Clinical candidate for cancer therapy, Pharmacol. Ther., 210 (2020) 107518.
[15] A. Hanzl, G.E. Winter, Targeted protein degradation: current and future challenges, Curr. Opin. Chem. Biol., 56 (2020) 35-41.
[16] Y.-W. Wang, L. Lan, M. Wang, J.-Y. Zhang, Y.-H. Gao, L. Shi, L.-P. Sun, PROTACS: A technology with a gold rush-like atmosphere, Eur. J. Med. Chem., 247 (2023) 115037.
[17] A.-H.M. Mustafa, O.H. Krämer, Pharmacological Modulation of the Crosstalk between Aberrant Janus Kinase Signaling and Epigenetic Modifiers of the Histone Deacetylase Family to Treat Cancer, Pharmacol. Rev., 75 (2023) 35-61.
[18] B. Sun, W. Fiskus, Y. Qian, K. Rajapakshe, K. Raina, K. Coleman, A. Crew, A. Shen, D. Saenz, C. Mill, BET protein proteolysis targeting chimera (PROTAC) exerts potent lethal activity against mantle cell lymphoma cells, Leukemia, 32 (2018) 343-352.
[19] G.M. Burslem, B.E. Smith, A.C. Lai, S. Jaime-Figueroa, D.C. McQuaid, D.P. Bondeson, M. Toure, H. Dong, Y. Qian, J. Wang, The advantages of targeted protein degradation over inhibition: an RTK case study, Cell chemical biology, 25 (2018) 67-77. e63.
[20] M. He, C. Cao, Z. Ni, Y. Liu, P. Song, S. Hao, Y. He, X. Sun, Y. Rao, PROTACs: great opportunities for academia and industry (an update from 2020 to 2021), Signal Transduction and Targeted Therapy, 7 (2022) 181.
[21] D. Chirnomas, K.R. Hornberger, C.M. Crews, Protein degraders enter the clinic—a new approach to cancer therapy, Nature Reviews Clinical Oncology, 20 (2023) 265-278.
[22] D. Menolfi, S. Zha, ATM, ATR and DNA-PKcs kinases—the lessons from the mouse models: inhibition≠ deletion, Cell & Bioscience, 10 (2020) 1-15.

[23] Y. Lu, M. Knapp, K. Crawford, R. Warne, R. Elling, K. Yan, M. Doyle, G. Pardee, L. Zhang, S. Ma, M. Mamo, E. Ornelas, Y. Pan, D. Bussiere, J. Jansen, I. Zaror, A. Lai, P. Barsanti, J. Sim, Rationally Designed PI3Kα Mutants to Mimic ATR and Their Use to Understand Binding Specificity of ATR Inhibitors, JMBio, 429 (2017) 1684-1704.
[24] T. Ishiyama, M. Murata, N. Miyaura, Palladium (0)-catalyzed cross-coupling reaction of alkoxydiboron with haloarenes: a direct procedure for arylboronic esters, The Journal of Organic Chemistry, 60 (1995) 7508-7510.
[25] C.M. Camacho, M.G. Pizzio, D.L. Roces, D.B. Boggián, E.G. Mata, Y. Bellizzi, E. Barrionuevo, V.C. Blank, L.P. Roguin, Design, synthesis and cytotoxic evaluation of a library of oxadiazole-containing hybrids, RSC advances, 11 (2021) 29741-29751.
[26] D.S. Mortensen, S.M. Perrin-Ninkovic, R. Harris, B.G.S. Lee, G. Shevlin, M. Hickman, G. Khambatta, R.R. Bisonette, K.E. Fultz, S. Sankar, Discovery and SAR exploration of a novel series of imidazo[4,5-b]pyrazin-2-ones as potent and selective mTOR kinase inhibitors, Bioorg. Med. Chem. Lett., 21 (2011) 6793-6799.
[27] X. Jiang, J. Zhou, Y. Wang, X. Liu, K. Xu, J. Xu, F. Feng, H. Sun, PROTACs suppression of GSK-3β, a crucial kinase in neurodegenerative diseases, Eur. J. Med. Chem., 210 (2021) 112949.
[28] B. Zhou, J. Hu, F. Xu, Z. Chen, L. Bai, E. Fernandez-Salas, M. Lin, L. Liu, C.-Y. Yang, Y. Zhao, Discovery of a small-molecule degrader of bromodomain and extra-terminal (BET) proteins with picomolar cellular potencies and capable of achieving tumor regression, J. Med. Chem., 61 (2018) 462-481.
[29] Y. Li, J. Yang, A. Aguilar, D. McEachern, S. Przybranowski, L. Liu, C.-Y. Yang, M. Wang, X. Han, S. Wang, Discovery of MD-224 as a First-in-Class, Highly Potent, and Efficacious Proteolysis Targeting Chimera Murine Double Minute 2 Degrader Capable of Achieving Complete and Durable Tumor Regression, J. Med. Chem., 62 (2019) 448-466.
[30] J. Zhang, J. Che, X. Luo, M. Wu, W. Kan, Y. Jin, H. Wang, A. Pang, C. Li, W. Huang, Structural feature analyzation strategies toward discovery of orally bioavailable PROTACs of Bruton's tyrosine kinase for the treatment of lymphoma, J. Med. Chem., 65 (2022) 9096-9125.
[31] J. Min, A. Mayasundari, F. Keramatnia, B. Jonchere, S.W. Yang, J. Jarusiewicz, M. Actis, S. Das, B. Young, J. Slavish, Phenyl-Glutarimides: Alternative Cereblon Binders for the Design of PROTACs, Angew. Chem. Int. Ed., 60 (2021) 26663-26670.
[32] X. Han, C. Wang, C. Qin, W. Xiang, E. Fernandez-Salas, C.-Y. Yang, M. Wang, L. Zhao, T. Xu, K. Chinnaswamy, Discovery of ARD-69 as a highly potent proteolysis targeting chimera (PROTAC) degrader of androgen receptor (AR) for the treatment of prostate cancer, J. Med. Chem., 62 (2019) 941-964.
[33] H. Schumacher, R. Smith, R. Williams, The metabolism of thalidomide: the fate of thalidomide and some of its hydrolysis products in various species, Br. J. Pharmacol. Chemother., 25 (1965) 338.
[34] R. Ashry, A.-H.M. Mustafa, K. Hausmann, M. Linnebacher, S. Strand, W. Sippl, M. Wirth, O.H. Krämer, NOXA Accentuates Apoptosis Induction by a Novel Histone Deacetylase Inhibitor, Cancers (Basel), 15 (2023) 3650.